

AD-A196 737

DTIC FILE COPY

4

OFFICE OF NAVAL RESEARCH

Contract N00014-87-K-0457

R&T Code 4134015—01

Technical Report No. 3

Solid-State  $^{29}\text{Si}$  NMR and Infrared Studies of the Reactions of Mono-  
and Polyfunctional Silanes with Zeolite Surfaces

by

+Thomas Bein, #Robert F. Carver, #Rodney D. Farlee, Galen D. Stucky

accepted for publication:  
Journal of the American Chemical Society

Department of Chemistry  
University of California  
Santa Barbara, California 93106

DTIC  
SELECTED  
JUN 16 1988  
CA  
H

+Department of Chemistry, University of New Mexico, Albuquerque, NM 87131

#Central Research and Development Department, E.I. du Pont de Nemours & Co.,  
Wilmington, DE 19898

Reproduction in whole or in part is permitted for any purpose of the United  
States Government

\*This document has been approved for public release and sale; its  
distribution is unlimited.

\*This statement should also appear in Item 10 of the Document Control Data-DD  
Form 1473. Copies of the form available from cognizant contract  
administration.

88 6 14 890

ADA196737

REPORT DOCUMENTATION PAGE		READ INSTRUCTIONS BEFORE COMPLETING FORM
1. REPORT NUMBER 3	2. GOVT ACCESSION NO.	3. RECIPIENT'S CATALOG NUMBER
4. TITLE (and Subtitle) Solid-State <sup>29</sup> NMR and infrared Studies of the Reactions of Mono- and Polyfunctional Silanes with Zeolite Surfaces.		5. TYPE OF REPORT & PERIOD COVERED Technical
		6. PERFORMING ORG. REPORT NUMBER
7. AUTHOR(s) Thomas' Bein, Robert F. Carver, Rodney D. Farlee, Galen D. Stucky.		8. CONTRACT OR GRANT NUMBER(s) N00014-87-K-0457
9. PERFORMING ORGANIZATION NAME AND ADDRESS Department of Chemistry University of California Santa Barbara, CA 93106		10. PROGRAM ELEMENT, PROJECT, TASK AREA & WORK UNIT NUMBERS
11. CONTROLLING OFFICE NAME AND ADDRESS		12. REPORT DATE May 1988
		13. NUMBER OF PAGES
14. MONITORING AGENCY NAME & ADDRESS (if different from Controlling Office)		15. SECURITY CLASS. (of this report) Unclassified
		15a. DECLASSIFICATION/DOWNGRADING SCHEDULE
16. DISTRIBUTION STATEMENT (of this Report)		
17. DISTRIBUTION STATEMENT (of the abstract entered in Block 20, if different from Report)		
18. SUPPLEMENTARY NOTES Accepted for publication in Journal of the American Chemical Society		
19. KEY WORDS (Continue on reverse side if necessary and identify by block number) NMR, zeolite, silanes, infrared, disorder.		
20. ABSTRACT (Continue on reverse side if necessary and identify by block number)		

# ABSTRACT

The combined use of  $^{29}\text{Si}$  magic-angle spinning NMR spectroscopy and in situ infrared techniques allows for the first time the determination of the intrazeolitic reaction products and details of the interaction of various silanes with zeolitic protons.

Alkoxy groups at  $\text{Me}_3\text{SiOMe}$  and  $\text{MeSi(OMe)}_3$  are readily lost to form hydroxy groups and then siloxane bridges to the zeolite framework. At elevated temperatures, alkyl groups are also split off from the silane, and more highly substituted siloxane species are generated which are anchored to the framework via two siloxane bridges.

Chloro groups are rapidly hydrolyzed by the surface hydroxy groups, and the resulting products follow the reaction pattern of the alkoxysilanes.

Hexamethyldisilazane and trimethylsilane do not react irreversibly with the zeolite hydroxyls at 295 K, but are as reactive as other silanes at 473 K. A major product with these silanes shows a unique NMR shift at about +40 ppm and is assigned to a Lewis-acid or strongly hydrogen-bonded association of the anchored silicon species with a framework metal.

Most of the reactions are more complex than those of halosilanes with the terminal hydroxyls of silica, indicating the extreme reactivity of bridged hydroxyl groups in zeolites.



Accession For	
NTIS GRA&I	<input checked="" type="checkbox"/>
DTIC TAB	<input type="checkbox"/>
Unannounced	<input type="checkbox"/>
Justification	
By	
Distribution/	
Availability Codes	
Dist	Avail and/or Special
A-1	

Solid-State  $^{29}\text{Si}$  NMR and Infrared Studies of the Reactions  
of Mono- and Polyfunctional Silanes with Zeolite Surfaces

Thomas Bein<sup>\*,a,b</sup>, Robert F. Carver<sup>b</sup>, Rodney D. Farlee<sup>b</sup>,  
and Galen D. Stucky<sup>c</sup>

Contribution from the Central Research and Development  
Department<sup>†</sup>, E.I. du Pont de Nemours and Company  
Experimental Station  
Wilmington, DE 19898, USA and the  
Department of Chemistry  
University of California  
Santa Barbara, CA 93106, USA

<sup>a</sup>Present address: Department of Chemistry, University of New Mexico,  
Albuquerque, NM 87131.

<sup>b</sup>DuPont

<sup>c</sup>UC Santa Barbara

<sup>†</sup>Contribution No: 4190

## ABSTRACT

The combined use of  $^{29}\text{Si}$  magic-angle spinning NMR spectroscopy and in situ infrared techniques allows for the first time the determination of the intrazeolitic reaction products and details of the interaction of various silanes with zeolitic protons.

Alkoxy groups at  $\text{Me}_3\text{SiOMe}$  and  $\text{MeSi(OMe)}_3$  are readily lost to form hydroxy groups and then siloxane bridges to the zeolite framework. At elevated temperatures, alkyl groups are also split off from the silane, and more highly substituted siloxane species are generated which are anchored to the framework via two siloxane bridges.

Chloro groups are rapidly hydrolyzed by the surface hydroxy groups, and the resulting products follow the reaction pattern of the alkoxysilanes.

Hexamethyldisilazane and trimethylsilane do not react irreversibly with the zeolite hydroxyls at 295 K, but are as reactive as other silanes at 473 K. A major product with these silanes shows a unique NMR shift at about +40 ppm and is assigned to a Lewis-acid or strongly hydrogen-bonded association of the anchored silicon species with a framework metal.

Most of the reactions are more complex than those of halosilanes with the terminal hydroxyls of silica, indicating the extreme reactivity of bridged hydroxyl groups in zeolites.

## INTRODUCTION

The chemical modification of zeolites has attracted considerable attention since these crystalline porous materials were introduced several decades ago. Ion exchange by transition metals and ammonium ions plays a major role to control catalytic and acidic properties. The complex zeolite structure is, however, by far not limited to modifications by these techniques, and recent work has focused on tailoring the hydrophobicity, adjust pore sizes, or specifically poison certain catalytic functions of the zeolite surface.

The intention of this study is to explore the possibility of "anchoring" certain molecules to the internal surface of the zeolite pore system. If reactions of this kind could be controlled, a general means would be available for the synthesis of fixed ligands, acids or other functional groups in the pore system. Unique catalytic applications of these systems are conceivable, for instance aimed at the stabilization of low valent transition metal species.

Silanes represent a well known class of reagents for the modification of oxide surfaces, and a number of studies deal with surface reactions of silanes with zeolites<sup>1-14</sup>.

Gravimetric and IR spectroscopic methods have been used to examine the reaction of alkylhalogenosilanes with dehydrated HY zeolite<sup>1</sup>. Above 500 K, zeolitic protons were found to react with both Si-Cl and Si-CH<sub>3</sub> bonds to form additional siloxane bridges, and byproducts HCl and CH<sub>4</sub>. High intrazeolitic concentrations of HCl destroyed the zeolite via attack at framework siloxane bonds.

Methane evolution was monitored upon reaction of tetramethyl silane with HY zeolite above 500 K<sup>2</sup>, and the formation of a siloxane bond between Me<sub>3</sub>Si- and the zeolite lattice was postulated. Silane, SiH<sub>4</sub>, has been used for the titration and silanation of hydroxyl groups in dealuminated mordenites<sup>3</sup>, under the assumption that the zeolite bridged hydroxyl groups produced stoichiometric amounts of hydrogen. The sorption behavior of the modified zeolites indicated pore-size narrowing and partial blocking of the mordenite channels<sup>4, 5</sup>, which has been applied for the encapsulation of noble gases in the zeolite pores<sup>6, 7</sup>. Vapor of Si(OMe)<sub>4</sub><sup>8</sup>, emulsions of alkylsilicones with water<sup>9</sup>, and a variety of functional alkyl silanes<sup>10</sup> have been reported to decrease the zeolite pore sizes by either narrowing the windows at the outer surface<sup>8</sup> or by internal coating of the pore system. Zeolite treatments with silanes have been shown to increase the hydrophobicity<sup>11</sup>, and similarly treated zeolites are reported as calcium exchangers in detergents<sup>12-14</sup>.

While the reactivity of polyfunctional silanes with zeolites has been established, only limited attempts have been undertaken to characterize the systems obtained by the various treatments, and the intrazeolite chemistry has either been derived by indirect methods<sup>1</sup> or has been speculated to involve tricoordinated oxygen as anchoring site for the silane<sup>10</sup>. In this study, a combination of solid-state magic angle spinning NMR (MAS NMR) and in situ infrared spectroscopy has been employed to elucidate the chemistry of silanes in the pore system of acid zeolites. MAS-NMR has recently been used for detailed studies on related reactions of silanes with the terminal hydroxyls of amorphous silica<sup>15-22</sup>.

Infrared spectroscopy as a complimentary technique contributes to the understanding of acid-base chemistry of oxide surfaces, and has been applied to differentiate between the reactivity of geminal and single silica hydroxyls towards hexamethyldisilazane and methyltrimethoxysilane<sup>24,25</sup>.

### <sup>29</sup>Si NMR

The <sup>29</sup>Si NMR chemical shift is a powerful tool for identifying various surface sites. Of interest in this work are the chemical shifts of silicon bonded to -Me, -OMe, -OH, and -Cl groups, and bonded to the silica or aluminosilicate surface by a bridging oxygen, as in a disiloxane (here denoted -OSi).

It has been known for some time that <sup>29</sup>Si chemical shifts can be related to the sum of the substituent electronegativities<sup>26</sup>. For substituents having low electronegativity (as in alkylsilanes), sigma bonding predominates; substitution with a ligand of higher electronegativity produces a downfield shift. If the substituents exhibit higher electronegativities (as in most siloxanes and all silicates) and have accessible pi orbitals, pi bonding is dominant; substitution with a ligand of higher electronegativity then produces an upfield shift.

Because of the competitive effects of sigma and pi bonding, the chemical shift is not a linear function over the full range of substituent electronegativities, and additive chemical parameters must be used with care. Sindorf and Maciel<sup>27</sup> have extracted relative substituent effects for -OR (R = alkyl), -OH, -Cl, and -OSi, and demonstrated that they are good



predictors of actual chemical shifts found for surface sites on derivatized silicas. Janes and Oldfield<sup>28</sup> have more recently described a predictive correlation of the chemical shifts of a wide range of silicates. These linear correlations are successful because these substituents all have high electronegativity relative to alkyl groups, and participate in pi bonding with Si.

Many of the species of interest in this work have substituent electronegativity sums in the range in which sigma and pi bonding compete as dominant effects on the chemical shift, making prediction of their shifts difficult. Because of the large body of relevant data available in the literature<sup>29,34</sup>, chemical shifts of essentially all the possible products can simply be compiled. Table 1 contains the <sup>29</sup>Si chemical shifts of various discrete molecules, surface sites, and solid silicates relevant to this work. These data are collected from the literature on <sup>29</sup>Si NMR of silane, siloxane and silicate solutions and derivatized silicas. It is important to note that mono-, di-, and trisubstitution are resolved in well defined <sup>29</sup>Si chemical shift regions. This allows a convenient definition of reaction products.

[Insert Table 1 near here]

For this reason, we find it useful to regard the species in Table 1 as substituted methylsilanes, by counting the number of substituents on Si which are not alkyl groups. These substituents (-Cl, -OH, -OMe, -OSi) are potentially reactive under conditions of modest acidity, such as during the hydrolysis and condensation of alkylsilicates, the self-condensation of silicate solutions, or the derivatization of silica by chlorosilanes. These

reactions will result in products described by the same degree of substitution borne by the reactants. In contrast, the high acidity of zeolites was found (vide infra) to be capable of increasing the degree of oxygen substitution by cleaving Si-C bonds.

The chemical shifts of discrete alkyl monosilicate species are not available because of their instability toward rapid condensation to higher silicates. However, one would expect that the shifts for the series  $\text{Si}(\text{OH})_n(\text{OMe})_{4-n}$  would all lie between -79 ppm ( $n=0$ )<sup>29,32</sup> and -74 ppm ( $n=4$ )<sup>29,31</sup>, if the substituent effects are assumed to be linearly additive.

Note that no silicate or mono- or poly-silane resonances with chemical shifts above +35 ppm have been reported ( $\text{Me}_3\text{SiF}$  is at +35 ppm<sup>29</sup>). Trimethylsilyl ligands on metals exhibit shifts above +35 ppm (e.g.  $(\text{Me}_3\text{Si})_2\text{Hg}$ , 64 ppm<sup>29</sup>). Several of the materials studied here exhibit a peak at +40 ppm. Since there are no known simple covalently bonded species which have this shift, we hypothesize that it arises from an ionic, Lewis acid-base interaction with the framework, such as  $\text{Me}_3\text{Si-Al}$  or  $\text{Me}_2\text{Si}(-\text{Al})(-\text{OSi})$ , or from hydrogen-bonding or protonation by the framework, as  $\text{H}^+-\text{Si}(\text{CH}_3)_3-\text{OSi}$ .

It should be noted that it appears that a small but consistent downfield shift is observed in the solid state relative to solution. Sindorf and Maciel<sup>27</sup> report an average "solid-state <sup>29</sup>Si chemical shift" difference of +7 ppm for trimethylsilyl groups bonded to a silica surface, relative to their

shift in solution. We find this value to vary between +2 and +7 ppm in the species studied here. This shift is not included in those data reported in Table 1 which were measured in solution.

For purposes of comparison with the work to be described below, it is useful to briefly summarize the sites produced by the reaction of chlorosilanes with the surface hydroxyls of silica, as determined from our previous studies<sup>21</sup> and elsewhere<sup>15-20,22,23</sup>.

Reaction of surface hydroxyls of silica with  $\text{Me}_3\text{SiCl}$  at moderate temperatures produces  $\text{Me}_3\text{Si-OSi}$  groups bonded to the surface.

$\text{Me}_2\text{SiCl}_2$  reacting with one hydroxyl will initially produce  $\text{Me}_2\text{Si}(\text{Cl})(\text{OSi})$  species. There are three possible steps for their further reaction:

- (1) react with a second surface hydroxyl to produce  $\text{Me}_2\text{Si}(\text{OSi})_2$  species.
- (2) In contact with water,  $-\text{Cl}$  will hydrolyze to produce  $-\text{OH}$ , which may further
- (3) crosslink with an adjacent  $-\text{Cl}$  to produce two  $\text{Me}_2\text{Si}(\text{OSi})_2$  sites, each bonded to one another and to the surface. The products of steps (1) and (3) cannot be distinguished by their  $^{29}\text{Si}$  NMR chemical shifts. The relative numbers of the two can, however, be indirectly determined by measuring the relative numbers of  $\text{Me}_2\text{Si}(\text{OSi})_2$  and  $\text{Me}_2\text{Si}(\text{Cl})(\text{OSi})$  present in  $^{29}\text{Si}$  NMR spectra of the initial, anhydrous samples<sup>27</sup>.

Reaction with trichlorosilanes is analogous, with the additional intermediates and increased amount of crosslinking that would be anticipated<sup>27</sup>.

The coverage of silicas can be calculated directly from the areas of the  $\text{Si(OH)}_2(\text{OSi})_2$ ,  $\text{Si(OH)(OSi)}_3$  and  $\text{Me}_3\text{Si(OSi)}$  resonances in  $^{29}\text{Si}$  CP-MAS spectra<sup>15,17,20,21</sup>. In zeolites, these effects are masked by signal from the bulk zeolite and cannot be differentiated from the external surface (except in highly siliceous zeolites such as silicalite).

## EXPERIMENTAL SECTION

### 1. Materials

Trimethylmethoxysilane, methyltrimethoxysilane, trimethylchlorosilane and hexamethyldisilazane (Strem Chemicals) were stored over sieve 4A without further purification. Gaseous trimethylsilane (Petrarch Systems) was used without purification.  $\text{NH}_4\text{Y}$  zeolite with the composition  $\text{Na}_8(\text{NH}_4)_{47}\text{Al}_{55}\text{Si}_{137}\text{O}_{384}\cdot n\text{H}_2\text{O}$  was obtained from Linde (LZ-Y62). Prior to use, the ammonium form of the zeolite was degassed by heating at a rate of 2 K/min. to 670 K, and maintained at 670 K for 12 hours under  $10^{-5}$  torr to yield the dry acid form (HY).

### 2. Methods

Samples for solid state NMR experiments were prepared as follows. Batches of dry HY were weighed into a small quartz holder, introduced into a tubular quartz reactor and evacuated at a greaseless vacuum line ( $10^{-5}$  torr) for 30 min. A degassed and frozen vial containing the silane was allowed to warm to 273 K and dosed manometrically onto the zeolite. After equilibrating for 120 min at 295 K, the sample was evacuated for 30 min, and weight changes were recorded in the drybox. The calculated loading (molecules of silanes per supercage, X/SC) is listed for each sample in the corresponding figure caption, based on equivalents of physisorbed silane. Heat treatments were done in the same reactor under vacuum, or under the vapor pressure of the silane, with a heating rate of 1 K/min. With trimethylsilane, an excess was dosed on the zeolite at a pressure of 50 torr.

The  $^{29}\text{Si}$  MAS-NMR spectra were obtained at 59.6 MHz on a Bruker CXP-300 instrument. Andrews type rotors were filled with ca. 200 mg of sample in the drybox and introduced into the NMR probe in a glovebag under flowing nitrogen. Dry nitrogen was used as the drive gas for the rotor to obtain spinning rates between 2 and 4 kHz. A  $30^\circ$  to  $90^\circ$  pulse with 10 s recycle time was used, depending on the  $T_1$ , to obtain quantitative spectra. Cross-polarization was not used, to ensure that mobile species would be observed quantitatively.  $^1\text{H}$ -decoupling time was 20 to 60 ms. Chemical shifts were referred to  $\text{Me}_4\text{Si}$ , using external hexamethyltrisiloxane in  $\text{CDCl}_3$  (-9.2 ppm) as secondary reference. No significant oxidation of the silanes was observed during the NMR experiments.

In situ infrared experiments were done with self-supporting zeolite wafers ( $5 \text{ mg/cm}^2$ ), compacted at  $100 \text{ kg/cm}^2$ , in a controlled-atmosphere cell with  $\text{CaF}_2$  windows connected to a Nicolet 50XB FT-IR spectrometer. Sample treatment was similar to that of the NMR samples, with the exception of shorter temperature cycles.

## RESULTS AND DISCUSSION.

### Trimethylmethoxysilane - NMR

$^{29}\text{Si}$  MAS NMR spectra of H-Y loaded with  $\text{Me}_3\text{SiOMe}$  vapor are shown in Figure 1A-4A. The major resonances are due to silicon in the zeolite framework having one Al and three Si neighbors at -98 ppm, and having four Si neighbors at -101.5 ppm. Throughout this study, the chemical shifts of these resonances are unchanged. Slight variations in the relative intensities of these resonances are observed, and reflect differences in the spin-lattice relaxation times of the framework Si sites in these dehydrated zeolites. The region of interest in this work spans the chemical shifts of silanes and siloxanes, and is expanded in Figures 1B-4B.

If dehydrated HY zeolite is saturated with vapor of  $\text{Me}_3\text{SiOMe}$  at 295 K, three new silicon species at 31, 20 and 10 ppm are observed in the  $^{29}\text{Si}$  MAS-NMR of the zeolite (Figure 1B). The species at 20 ppm (45 mol %) can be assigned either to the starting silane (17.7 ppm in solution) or to the hydrolysis product,  $\text{Me}_3\text{SiOH}$ , which has a predicted shift of 17 ppm (see Table I). These observations are summarized in Table II.

Trimethylsilyl groups bonded to the surface,  $\text{Me}_3\text{SiOSi}$ , are observed at 10 ppm (38%). The third peak at 31 ppm appears at an unusual position for oxygen-bonded silicon and will be labeled a yet undefined Si-zeolite Lewis-acid adduct (e.g.  $\text{T}_2\text{O} \cdots \text{H}(\text{O}(\text{Me})\text{SiMe}_3)$ ) and is discussed further in following sections.

Upon degassing this material at 403 K under vacuum, striking changes occur in the  $^{29}\text{Si}$  NMR spectrum. None of the original silanes seen between 30 and 10 ppm survive this treatment, and new resonances at 0 (28%), -11 (54%) and -20 ppm (18%) are observed (Figure 2A, B).

These data are consistent with the generation of  $\text{Me}_2\text{Si}(\text{OMe})_2$  (-2 ppm), and two products of condensation with the zeolite hydroxyls:  $\text{Me}_2\text{Si}(\text{OMe})\text{OSi}$  and  $\text{Me}_2\text{Si}(\text{OSi})_2$  (Scheme 2).

Further heating at higher temperature (523 K) causes further condensation of the dimethylsiloxane species. The intensity of the peak at -11 ppm drops from 54 to 29%, that at -20 ppm increases from 18 to 48 mol % (Figure 3A, B). Additional peaks are observed in the region of a spinning sideband of the zeolite resonance (-64 ppm); the peak at -56 ppm (Figure 3A) is assigned to  $\text{MeSi}(\text{OSi})_3$  and/or  $\text{MeSi}(\text{OMe})(\text{OSi})_2$  produced by protolysis of  $\text{Me}_2\text{Si}(\text{OSi})_2$ .

If dehydrated HY is equilibrated with vapor of  $\text{Me}_3\text{SiOMe}$  at 473 K, more pronounced condensation is observed compared to the vacuum treatments (Figure 4A, B). The major intensity is now represented by methyltrisiloxane species  $\text{MeSi}(\text{OMe})(\text{OSi})_2$  and/or  $\text{MeSi}(\text{OSi})_3$  at -57 ppm(41%), in addition to smaller amounts of disubstituted ( $\text{Me}_2\text{Si}(\text{OSi})_2$ , -18 ppm (32%)) and non-bonded material (TMS or  $\text{Me}_2\text{Si}(\text{OMe})_2$ , 1 ppm (18%)).



### Trimethylmethoxysilane - IR

The IR spectrum of a self-supporting wafer of  $\text{NH}_4\text{Y}$  zeolite, degassed at 670 K for 14 hrs under vacuum, is shown in Figure 5A. Three well-known hydroxyl groups can be distinguished: terminal Si-OH groups at the outer surface of the zeolite crystals ( $3740\text{ cm}^{-1}$ ), "supercage"  $\text{SiO(H)Al}$  hydroxyls at  $3640$  and "sodalite"  $\text{SiO(H)Al}$  at  $3540\text{ cm}^{-1}$ . The latter two species, depicted  $\text{SiO(H)Al}$ , are bridged hydroxyls, located in different framework positions in the Si-O-Al six-rings of the faujasite structure.

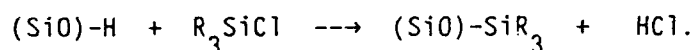
If the zeolite wafer is equilibrated with vapor of  $\text{Me}_3\text{SiOMe}$  and pumped off for 30 min, striking changes in the spectrum indicate an acid-base reaction between the zeolite hydroxyls and the silane (Figure 5B). The high frequency supercage hydroxyls are almost entirely consumed upon chemisorption, whereas the low frequency hydroxyls are essentially unaffected. In addition to the expected C-H stretching and bending vibrations of the silane ( $3000\text{-}2800$  and  $1480\text{-}1370\text{ cm}^{-1}$ ), two strong broad bands are observed at  $2425$  and  $1750\text{ cm}^{-1}$ . The former vibration is assigned to proton-stretching modes of protonated siloxane species, like  $\text{Me}_3\text{SiOH--OT}_2$ , that are protolysis products of the chemisorbed silane. The band around  $1750\text{ cm}^{-1}$  cannot be correlated to a specific species at the present time.

Treatment of the zeolite wafer with silane at 403 K for one hour results in dramatic changes (Figure 5C). In addition to the supercage hydroxyls, a large fraction of the previously inaccessible low frequency hydroxyls are also consumed. The broad bands at  $1750$  and  $2425\text{ cm}^{-1}$  are destroyed, and changes in the C-H stretch intensities at  $2860\text{ cm}^{-1}$  indicate the loss of certain species. Further treatment with silane vapor at elevated temperature (2 hours

at 473 K) causes continued consumption of the hydroxyl groups and formation of a new species at  $1455\text{ cm}^{-1}$  (Figure 5D). This mode is assigned to the methoxy group of the trisubstituted, framework anchored siloxane  $\text{MeSi(OMe)(OSi)}_2$  which is observed in the corresponding NMR experiment (Figure 4A, B).

#### Trimethylmethoxysilane - Discussion

Terminal hydroxyl groups on silica and alumina surfaces are well-established sites for surface modification reactions<sup>15-21</sup>. The straightforward reaction of these hydroxyls with halosilanes or triethoxy-substituted silanes produces Si-O-Si bridges, anchoring the respective silane by a nucleophilic substitution:

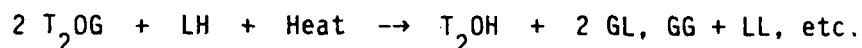
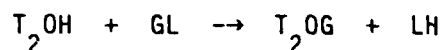


The major fraction of zeolite hydroxyl groups are of the bridged type. The weak bond between bridged oxygen and protons explains why acid zeolite surfaces show much higher acidity than the amorphous oxides.

On the other hand, a three-coordinated oxygen cannot be expected to provide a strong bond between a functional group and the zeolite framework. Two possibilities represent the major reaction pathways in this situation:

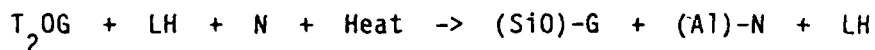
1. The bonding to the bridged oxygen is weak. Upon thermal excitation, the functional group G will then desorb, condense with a second one or will react to give other products:

(SiO(H)Al will be abbreviated by  $T_2OH$ )



A comparable situation is represented by the chemisorption of tricoordinated phosphines in dehydrated, acid faujasite: At room temperature, the phosphine is protonated and remains adsorbed as phosphonium ion. This reaction is reversible, and the phosphine can be desorbed at elevated temperature, restoring the zeolite hydroxyl groups<sup>35</sup>.

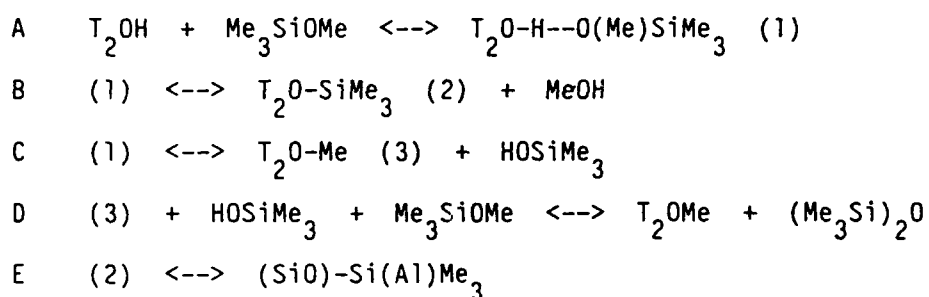
2) The second pathway is a condensation reaction between the functional group and the bridged oxygens. It has to be expected that the original Si-O-Al oxygen bridge will be destroyed during this reaction, leaving a tricoordinated framework metal - e.g. aluminum - which is likely to coordinate to other nucleophiles N present in the zeolite pore system.



One significant difference exists between the degrees of reversibility: Weak bonding (path 1) restores the zeolite hydroxyls upon degassing; whereas breaking the Si-O-Al oxygen bridge (path 2) leads to irreversible consumption of protons upon degassing. Infrared studies of the hydroxyl region during degassing experiments can provide evidence for these alternatives.

If the above considerations are applied to the spectroscopic results of the  $\text{Me}_3\text{SiOMe}/\text{HY}$  system, the following conclusions can be drawn (for the assignments of chemical shifts, the convention is: predicted value/observed value, in ppm):

Upon adsorption in HY at 295 K, the silane is protonated by all available supercage protons, most likely at the methoxy-oxygen:



Quantitative data on the preferred reaction pathways of this system can not be derived from the present experimental results because it is not possible to determine the concentration of all the species involved.

There is, however, evidence for the formation of  $\text{Me}_3\text{SiOSi}$  (10 ppm) and possibly  $\text{Me}_3\text{SiOH}$  (+17 ppm).  $(\text{Me}_3\text{Si})_2\text{O}$  might also be present at 10 ppm (the solution chemical shift is 6.8 ppm). The upfield species observed at 31 ppm can be interpreted as evidence for the oxygen-bridge breaking reaction E or, alternatively, the hydrogen-bonded starting silane (A) as shown in Scheme 1. Inserting the Si of the silane into the  $\text{SiOAl}$  bridge generates a direct Si-metal coordination that typically shows higher upfield shifts<sup>24</sup>. Assignment of this resonance will be discussed further in a following section.

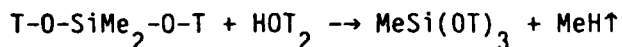
Additional evidence for the unstable, intermediate  $T_2O-H--O(Me)SiMe_3$  (reaction A) comes from the infrared spectra: At 295 K, a strong, broad band at  $2425\text{ cm}^{-1}$  indicates a hydrogen bond that disappears upon degassing at higher temperatures. The conclusions drawn from the above discussion are summarized in Scheme 1.

Heating at 403 K removes the unstable products and intermediates from the zeolite. None of the previous species remain, and the NMR data allow to conclude that di- and trisubstituted siloxanes are formed.

At elevated temperatures, additional protons are delivered from non-accessible sites into the supercage, as indicated by IR spectroscopy. At this stage, methyl groups are split off from the silane. This behavior is unknown with silica supports and points to the strong acidity of the zeolite. One reaction path proposed is the acid catalyzed methyl group substitution at the framework bonded monosiloxane (Scheme 2). A major product at elevated temperatures is  $Me_2Si(OMe)OSi$ , which is proposed to be generated by reaction with MeOH in the cage system (Scheme 2).

The product spectrum at higher degassing temperatures (523 K) confirms the trends observed at 403 K:

The higher condensation produce  $Me_2Si(OSi)_2$  becomes more pronounced, and an additional trisubstituted species  $MeSi(OSi)_3$  grows in:



The nature of the zeolite support does not allow to determine quaternary

siloxanes in the NMR because the bulk resonance from the zeolite appears at similar chemical shifts as would the reaction products. These products can therefore not be excluded from the reaction scheme.

If vapor of  $\text{Me}_3\text{SiOMe}$  is equilibrated with HY at 473 K, similar products as under vacuum degassing are observed. The trisubstituted species dominate with 41 mol %, followed by the disubstituted product (32%) and the non-bonded species with a shift of 1 ppm ( $\text{Me}_2\text{Si}(\text{OMe})_2$  or TMS). The species  $\text{Me}_2\text{Si}(\text{OMe})(\text{OSi})$  appears to be unstable under higher partial pressures of the starting material and is not detected here.

#### Methyltrimethoxysilane - NMR

At least four new silicon species are observed in the  $^{29}\text{Si}$  NMR of HY upon equilibration with  $\text{MeSi}(\text{OMe})_3$  at 295 K. New peaks appear at 18, 8, -38, -46 and -57 ppm (Figure 6A, B). These observations are summarized in Table III.

The species at 18 ppm is assigned to  $\text{Me}_3\text{SiOMe}$ , and the shoulder at 8 ppm appears to be the corresponding condensation product with the zeolite  $\text{Me}_3\text{Si}(\text{OSi})$ . The starting material  $\text{MeSi}(\text{OMe})_3$  is observed as a shoulder at -38 ppm.

The major component of the spectrum at -46 ppm (53%) can be assigned to the monosubstituted starting silane,  $\text{MeSi}(\text{OMe})_2\text{OSi}$ . The resonance at -57 ppm is due to disubstituted product,  $\text{MeSi}(\text{OMe})(\text{OSi})_2$  (Scheme 3).

Upon degassing this material at 403 K under vacuum, a gradual shift of intensities in favor of the higher condensation products is observed (Figure 7). The anchored trimethyl species  $\text{Me}_3\text{SiOSi}$  (12 ppm, 21%) is still present, but the starting material is completely consumed by further protolysis and condensation. The heat treatment transforms the major fraction of the silane into methoxymethylsilyl groups,  $\text{MeSi(OMe)(OSi)}_2$ , at -56 ppm (53%), in addition to  $\text{MeSi(OMe)}_2(\text{OSi})$ .

#### Methyltrimethoxysilane - IR

Saturation of the dehydrated zeolite wafer (Figure 8A) with  $\text{MeSi(OMe)}_3$  at 295 K causes dramatic changes in the IR spectrum. An extremely strong and broad absorption appears between 3600 and 2600  $\text{cm}^{-1}$  (Figure 8B). The only structure visible on this absorption is a shoulder at 3525 (sodalite hydroxyl) and the C-H stretch bands at 3000-2800  $\text{cm}^{-1}$ . The broad absorption is assigned to a convolution of free hydroxyl and intermolecular bonded hydroxyl vibrations, most likely due to interactions of the byproduct MeOH with the zeolite hydroxyls.

At 2425  $\text{cm}^{-1}$ , a strong, symmetric absorption appears that is assigned to weaker hydroxyl bonds with the starting material (Scheme 3) as observed with  $\text{Me}_3\text{SiOMe}$  (Figure 5). C-H bending modes are observed for methoxy (1460, 1450) and for methyl groups at the silicon (1405, 1275  $\text{cm}^{-1}$ ).

If the wafer is equilibrated with silane at 403 K for one hour and degassed again, a number of bands decrease in intensity (Figure 8C). The hydroxyl bridge mode at 2425  $\text{cm}^{-1}$  as well as the broad hydroxyl absorption

are diminished and the "sodalite" hydroxyl of the zeolite is partially restored. C-H bending modes due to methoxy ( $1450\text{ cm}^{-1}$ ) are significantly reduced in intensity.

Vapor treatment and evacuation at 473 K results in a gradual loss of intensity of most of the bands (Figure 8D). The broad hydroxyl absorption is still a predominant feature in this spectrum; whereas the relative intensity of methoxy versus methyl is further decreased.

It should be noted that hydrolyzable groups at silanes do not always lead to a complete consumption of zeolite hydroxyls. Of the three examples considered here, only the monomethoxysilane  $\text{Me}_3\text{SiOMe}$  shows an increasing tendency to destroy the inaccessible "sodalite" protons, whereas  $\text{Me}_3\text{SiCl}$  and  $\text{MeSi(OMe)}_3$  leave these groups essentially unaffected.

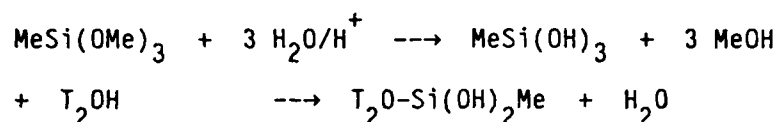
#### Methyltrimethoxysilane - Discussion

The reactions of the trimethoxy silane can be understood in terms of protolysis, methyl split-off and condensation with the framework, as in the case of  $\text{Me}_3\text{SiOMe}$ :

- A minor fraction of unreacted starting material is detected upon chemisorption at room temperature. This component disappears upon treatment at 403 K.
- Reaction of the methoxy groups with zeolite protons causes breaking of the oxygen-silicon bond to give framework bonded siloxanes (Scheme 3).

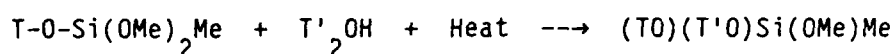


Residual water in the zeolite is expected to play an additional role in this process by prompting acid-catalyzed hydrolysis:



We assume the generation of hydroxysilanes, based on the very strong hydroxyl absorption in the IR (Figure 8B).

- Degassing the  $\text{MeSi(OMe)}_3/\text{HY}$  adduct at 403 K favors the formation of higher condensation products: The concentration of the  $\text{MeSi(OMe)(OSi)}_2$  species grows from 19 to 53 mol %, at the expense of starting material and singly bonded silane.



The concomitant consumption of zeolite hydroxyl groups is clearly demonstrated in the IR experiment: both low and high frequency hydroxyl bands decrease in intensity upon degassing (Figure 8C, D) at elevated temperature. Inspection of these spectra shows also a relative decrease of methoxy versus methyl groups upon degassing. This effect is interpreted as being due to direct substitution of methoxy- by hydroxyl-groups as MeOH or due to desorption of other methoxy species like MeOMe.

- As with  $\text{Me}_3\text{SiOMe}$ , the chemisorption of the trimethoxysilane in acid zeolite proves to be irreversible: Supercage hydroxyls are not restored at higher degassing temperatures (Figure 8C, D), indicating that stoichiometric substitution reactions take place, rather than acid catalyzed hydrolysis of the adsorbed silane.

### Trimethylchlorosilane - NMR

Saturation of HY with vapor of  $\text{Me}_3\text{SiCl}$  at 295 K generates four new silicon species in the  $^{29}\text{Si}$  NMR of the zeolite (Table IV, Figure 9A, B). The component at 21 ppm (42%) is assigned to  $\text{Me}_3\text{SiOH}$  (pred. 17 ppm). The resonance at 12 ppm (24%) is assigned to trimethylsiloxy groups, and the broad resonance between -5 and -10 ppm to dimethylsiloxy groups, both bonded to the zeolite (Scheme 4A). An alternative assignment of the 13 ppm resonance to  $\text{MeSiCl}_3$  (pred. 12 ppm) is not favored for two reasons: the high reactivity of the Si-Cl bond renders a survival at higher temperatures unlikely (see below), and similar resonances have been found in the  $\text{HY/MeSi(OMe)}_3$  system, in which no -Cl is present.

The sample also exhibits a peak at 40 ppm (17%). Assignment of this resonance will be discussed further in the following sections.

If this material is degassed at 403 K, a moderate change in peak intensities is observed (Figure 10A, B). The broad resonance at -5 to -10 ppm is replaced by a stronger peak at -9 ppm (34%) which is assigned to dimethylhydroxysilyl groups anchored to the zeolite framework. The species at 41 and 13 ppm remain essentially unchanged, whereas the original peak at 21 ppm, assigned to  $\text{Me}_3\text{SiOH}$ , is consumed to reveal an additional peak at 27 ppm. This species is also present in the starting material as a shoulder and most likely represents unreacted  $\text{Me}_3\text{SiCl}$  (pred. 30 ppm) (Scheme 4B).

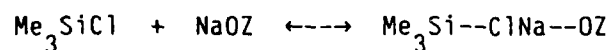
A more severe treatment of the zeolite with silane vapor at 473 K gives rise to a different product pattern (Figure 11A, B): The higher partial pressure of the starting material causes a high concentration of the framework-anchored  $\text{Me}_3\text{Si(OSi)}$  at about 7 ppm (37%).

Disubstituted species, for instance  $\text{Me}_2\text{Si(OH)(OSi)}$  are observed in the spectral region between -7 and -15 ppm, and represent 33% of the total intensity.

Trisubstituted siloxanes are generated in substantial amounts under the high partial pressure conditions; species with resonances between -51 and -59 ppm (e.g.  $\text{MeSi(OH)(OSi)}_2$ ) account for 30% of the silicon loading.

Chemisorption experiments with  $\text{Me}_3\text{SiCl}$  in non-acidic NaY support provide further evidence as to the nature of the acid reaction products (Figure 12A, B): The predominant species is a resonance at 38 ppm (77%), accompanied by smaller amounts of  $\text{Me}_3\text{SiOMe}$  at 18 ppm (14%) and  $\text{Me}_3\text{Si(OSi)}$  at 6 ppm (9%).

Since the chemical shift of  $\text{Me}_3\text{SiCl}$  is 30 ppm, the peak at 38 ppm is unlikely to represent the unreacted starting material. This species is proposed to be due to an association between the zeolite sodium ions and the silane:



(OZ, zeolite)

This product also arises from the other silanes studied here and will be discussed further in the following sections.

#### Trimethylchlorosilane - IR

If a dehydrated wafer of HY is equilibrated with  $\text{Me}_3\text{SiCl}$  at 295 K, a consumption of the major fraction of supercage hydroxyls is observed as with the other silanes under study (Figure 13B). A major difference to the former systems is the high frequency band between 3500 and 3100  $\text{cm}^{-1}$ , indicating hydroxyl bridges of moderate strength. This band can be understood as being due to a Si-Cl-H bridge in  $\text{Me}_3\text{SiCl}\cdots\text{HOZ}$ .

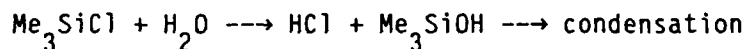
An additional hydrogen bond is represented by the band at 2425  $\text{cm}^{-1}$ . This band is found with all silanes studied. This suggests the formation of a common intermediate, probably with a Si-OH $\cdots$ OT<sub>2</sub> bond. Free  $\text{Me}_3\text{SiH}$  shows a  $\nu(\text{Si-H})$  at 2125  $\text{cm}^{-1}$ . No HCl (2885  $\text{cm}^{-1}$ ) is detected in the IR of the gas phase equilibrated with the zeolite. The C-H stretching and bending (1410 and 1260  $\text{cm}^{-1}$ ) frequencies resemble those of neat  $\text{Me}_3\text{SiCl}$ , indicating that the  $\text{Me}_3\text{Si}$  unit is intact.

Treatment of the zeolite wafer with silane at 403 K and degassing partially removes both the broad, bridged-hydroxyl band between 3500 and 3100  $\text{cm}^{-1}$  and the hydrogen band at 2425  $\text{cm}^{-1}$  (Figure 13C). This observation is indicative of increasing condensation reactions that are still more pronounced if the treatment is done at 473 K (Figure 13D).

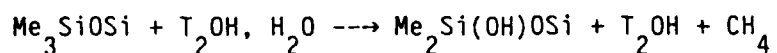
### Trimethylchlorosilane - Discussion

In order to account for the reactivity of the chloro silane in the zeolite cage system, the following reaction pathways should be considered:

- Traces of residual water in the pores of the zeolite, even if only present at the 0.2 wt.% level (or 2-3 molecules per unit cell) can hydrolyze noticeable fractions of the silane. A typical loading with silane, after 30 min. degassing at 295 K, corresponds to 10 molecules per unit cell or 1.2/supercage.



- Protolysis of the Si-Cl bond by zeolite hydroxyls to anchor the silane to the framework.
- Acid catalyzed Si-C bond cleavage to form more highly substituted siloxane species that can either oligomerize or form oxygen bridges with the framework.



The reactivity of  $\text{Me}_3\text{SiCl}$  with acid zeolite is understood in terms of these reaction pathways.

Chemisorption at 295 K produces a predominant fraction of monohydroxy substituted silane due to reaction with HCl. A smaller fraction of

framework-anchored  $\text{Me}_3\text{SiOSi}$  and  $\text{Me}_2\text{Si}(\text{OH})\text{OSi}$  is observed, and there is evidence for a Lewis adduct with the framework (assignment of the 41 ppm resonance is discussed in a later section).

Treatments at higher temperatures favor the formation of disubstituted siloxanes. Under a vapor pressure of chlorosilane at 470 K, trisubstituted condensation products with the framework are also produced. If the silane is absorbed in dehydrated NaY zeolite, the major product is probably the same Lewis-adduct as observed with HY.

It is clear that the intrazeolite environment is extremely reactive and favors the formation of functionalized silanes.

#### Trimethylsilane - NMR

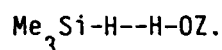
Dehydrated HY zeolite, equilibrated with  $\text{Me}_3\text{SiH}$  vapor at 295 K for 120 minutes, followed by evacuation for 30 minutes, exhibits no  $^{29}\text{Si}$  NMR signal in the silane or siloxane regions of the spectrum. The quantity of physisorbed silane is apparently too small to be detected in the  $^{29}\text{Si}$  NMR.

If the silane treatment is carried out at 473 K, however, two distinct products are identified in the NMR (Table V, Figure 16B). The major product is found at +41 ppm (60%). A second species at -2 ppm is due to  $\text{Me}_4\text{Si}$  or  $\text{Me}_2\text{Si}(\text{OMe})_2$ . The starting material (-15.5 ppm) is not detected in this spectrum, indicating complete intrazeolitic conversion of the silane.

### Trimethylsilane - IR

A dehydrated wafer of HY (Figure 17A) shows formation of a hydroxyl bond with  $\text{Me}_3\text{SiH}$  if equilibrated at 295 K (Figure 17B). The spectrum also shows a splitting of the Si-H vibration (gas phase  $2125\text{ cm}^{-1}$ ) into modes at 2050 and  $2125\text{ cm}^{-1}$ , as well as a weaker band at about  $2425\text{ cm}^{-1}$ .

The high frequency hydroxyl band at  $3640\text{ cm}^{-1}$  is reduced to a shoulder, and a broad band between  $3500$  and  $3200\text{ cm}^{-1}$  indicates a hydroxyl bridge with the adsorbed silane. This hydroxyl bridge is believed to generate the low frequency part of the  $\nu(\text{Si-H})$  vibration at  $2050\text{ cm}^{-1}$ :



If the silane gas is pumped off from the zeolite at 295 K, the supercage hydroxyl is almost completely restored in contrast to the other silanes studied. Only minor concentrations of C-H bands and the "protonated" species at  $2425\text{ cm}^{-1}$  remain, and the intact silane is completely removed as shown by the disappearance of the Si-H band (Figure 17C).

Silane treatment at 403 K changes the situation significantly (Figure 17D): only one  $\nu(\text{Si-H})$  from the zeolite-adsorbed silane is observed. This observation indicates that no free hydroxyls remain available for H-bonding in the zeolite. If the silane is pumped off after this treatment, the zeolite hydroxyls are not restored and the intensity of the C-H bands grows stronger (Figure 17E). Treatment with the silane at 473 K further consumes part of the zeolite hydroxyls (Figure 17F).

It is obvious that the consumption of hydroxyls is accompanied by a growing deposition of methyl species, indicating a framework anchoring reaction as with the other silanes.

#### Trimethylsilane - Discussion

If the spectroscopic observations reported for trimethylsilane are compared to those for the other silanes, a general relation appears to exist between the reactivity of the silane towards hydrolysis and the complexity of the product spectrum. The less reactive silane,  $\text{Me}_3\text{SiH}$ , generates a less complicated spectrum, and decreasing reactivity also favors formation of the unique product with a silicon shift at +41 ppm.

It is clear that trimethylsilane in acidic Y does not form oxygen-substituted siloxanes, with oxygen bridges anchored to the zeolite framework. The predominant species at 41 ppm is obtained at elevated reaction temperature. Several observations regarding this resonance are summarized below.

(a) Resonances with comparable chemical shift are observed after exposure to  $\text{Me}_3\text{SiOMe}$  (31 ppm) and to  $\text{Me}_3\text{SiCl}$  (40 ppm), but are not formed from  $\text{MeSi(OMe)}_3$ . This suggests that the species is a substituted trimethylsilyl group.

(b) Its formation is associated with the observation of  $\text{Me}_3\text{SiOMe}$  or  $\text{Me}_2\text{Si(OMe)}_2$  in the  $^{29}\text{Si}$  NMR spectrum.

(c) Appearance of this NMR resonance is not correlated with the appearance of any new feature in the IR spectra of this series of samples, but does correlate with loss of intensity of the zeolite hydroxyls bands.

(d) The chemical shift value excludes all of the species listed in Table I.



In fact, no tetravalent silanes or siloxanes having -H, -Cl, -Me, or -OMe ligands exhibit shifts this far to low field.

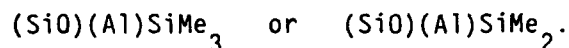
(e) The chemical shift correlations discussed earlier<sup>26, 28</sup> allow us to exclude the presence of a pi-bonding, electronegative ligand on Si, as this would move the chemical shift upfield into the range encompassed by the species listed in Table I.

(f) These same chemical shift correlations predict that a ligand which has higher electronegativity than -Me and which is capable of only sigma bonding, and not pi bonding interactions with Si, will produce a downfield shift like that observed.

(g) Trimethylsilyl ligands on metals have shifts that are not encompassed by these chemical shift correlations of simple silanes and siloxanes, but are known to exhibit chemical shifts above +35 ppm (e.g.  $(\text{Me}_3\text{Si})_2\text{Hg}$ , + 64 ppm).

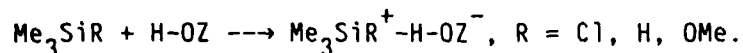
These observations do not lead to a definite assignment for this resonance, but three possibilities are listed below.

(a) A silane-Lewis acid adduct, with a direct Si-metal bond, like

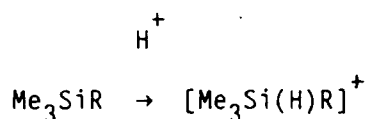


This proposed species is also consistent with a proton-consuming reaction, which is indicated by the loss of intensity due to zeolite hydroxyls in the IR spectra.

(b) Reaction with acidic zeolite hydroxyls to form a strongly hydrogen-bonded silane, with partial positive charge on Si, as



(c) It seems that the three starting silanes produce a single, identical product with a <sup>29</sup>Si shift near +40 ppm. One possible common product is the pentacoordinate silanium species below:



This species cannot, however, be identified unambiguously in the present study.

The new IR absorption observed at  $2050 \text{ cm}^{-1}$  is formed at room temperature in the acid zeolite. Its instability is reflected by the fact that it is completely destroyed upon heating. It appears at lower frequency than the physisorbed silane, which is observed at  $2125 \text{ cm}^{-1}$ , reflecting a weakening of the Si-H bonds. The broadening and absence of rotational bands in both the  $2050$  and  $2125 \text{ cm}^{-1}$  lines indicates strong adsorption to the zeolite surface.

The  $2050 \text{ cm}^{-1}$  absorption may be attributed either to strong physisorption of  $\text{Me}_3\text{SiH}$  at a specific site in the supercage, or to the formation of trimethylsilanium ion,  $\text{Me}_3\text{SiH}_2^+$ , bonded to the zeolite surface, by protonation of the silane by the acidic hydroxyls of the zeolite. Silanium ions have been observed in the gas phase by ion cyclotron resonance<sup>36</sup>. They are formed by proton transfer to  $\text{SiH}_4$  from  $\text{NH}_2^+$ ,  $\text{CH}_5^+$ ,  $\text{C}_2\text{H}_3^+$ ,  $\text{C}_2\text{H}_6^+$ , or  $\text{C}_2\text{H}_8^+$ .  $\text{SiH}_5^+$  is expected to be more stable than  $\text{CH}_5^+$ <sup>37</sup>.

#### Hexamethyldisilazane - NMR

If dehydrated HY zeolite is equilibrated with vapor of  $(\text{Me}_3\text{Si})_2\text{NH}$  at 295 K and degassed for 30 min., the retained amount of reaction products is too small to be detected in the  $^{29}\text{Si}$  MAS NMR spectrum.

The situation changes drastically if the equilibration temperature is raised to 473 K. After degassing the sample, the  $^{29}\text{Si}$  NMR indicates the formation of at least three new species in addition to the zeolite resonances at -98 and -101.6 ppm. No starting material (2.4 ppm) is detected after this treatment (Table V, Figure 14A, B).

Resonances at +10 and -14 ppm are assigned to  $\text{Me}_3\text{SiOSi}$  and  $\text{Me}_2\text{Si}(\text{OSi})_2$  species anchored to the zeolite framework (Scheme 5).

The predominant species is observed at +41 ppm (38%), and its assignment to a Lewis-adduct is discussed in the preceding section.

#### Hexamethyldisilazane - IR

Infrared in situ studies provide further evidence for the intrazeolite chemistry of  $(\text{Me}_3\text{Si})_2\text{NH}$ . If a wafer of dehydrated HY (Figure 15A) is saturated with the silazane, almost no interaction with the zeolitic hydroxyls at 3640 and 3540  $\text{cm}^{-1}$ , except the terminal SiOH at 3745  $\text{cm}^{-1}$ , is detected (Figure 15B). This is in strong contrast to all other silanes studied. A new high frequency band at 3400  $\text{cm}^{-1}$  is assigned to the  $\nu(\text{N-H})$  and the broad bands at 1500 - 1400  $\text{cm}^{-1}$  to the corresponding N-H bending vibrations. A very broad absorption between 3400 and 2400  $\text{cm}^{-1}$  is due to intermolecular N-H hydrogen bridges. Hydroxyl bridges can be excluded since the zeolite hydroxyls remain unaffected by the chemisorption.

If the zeolite wafer is saturated with silazane again at 403 K, the zeolite hydroxyls now are almost completely destroyed (Figure 15C). Both hydroxyl bands are concomitantly reduced to about 20% of the starting

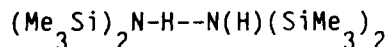
intensity, indicating that either sodalite protons have traveled into the supercage or that a small reaction product like  $\text{NH}_3$  gained access into the sodalite cage.

The  $\nu(\text{N-H})$  band at  $3400 \text{ cm}^{-1}$  is significantly diminished, probably due to reaction with the zeolite hydroxyls. A strong broad band at  $1430 \text{ cm}^{-1}$  is assigned to ammonium ions formed upon protonation by the acid zeolite. The  $\delta(\text{C-H})$  band at  $1260 \text{ cm}^{-1}$  (due to  $\text{CH}_3\text{Si}$ ) grows significantly upon vapor treatment at 403 K. This provides evidence for the anchoring reaction as indicated by the NMR results.

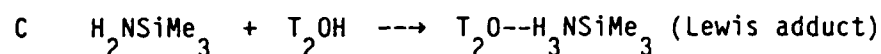
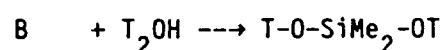
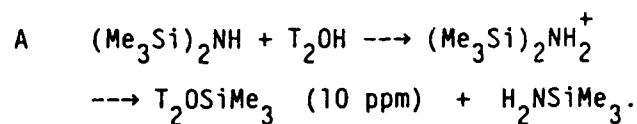
Silazane treatment at 473 K pronounces the reactions observed at 403 K (Figure 150). Zeolite hydroxyls and the  $\nu(\text{N-H})$  band are further consumed, the absorption due to bridged N-H and O-H diminishes, together with the ammonium band at  $1430 \text{ cm}^{-1}$ . The only peaks to grow are C-H stretch and bending vibrations. These observations can be summarized in pronounced anchoring of  $\text{Me}_3\text{Si-}$  units and degassing of other reaction products like  $\text{NH}_3$ .

#### Hexamethyldisilazane - Discussion

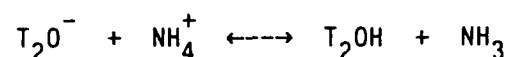
The reactivity of  $(\text{Me}_3\text{Si})_2\text{NH}$  in acid Y zeolite is lower than that of methoxy- and chlorosilanes. This is shown in the in situ IR by the intact zeolite hydroxyls after adsorption at 295 K. Strong intermolecular N-H bridges characterize the intrazeolite environment of the silazane:



At elevated temperatures, the zeolite hydroxyls do react almost to completion with the silazane, generating several protolysis products. NMR and IR data are consistent with the following reactions:



Ammonia, the protolysis product from the first sequence, is in a temperature-dependent equilibrium with the zeolite hydroxyls:



At higher temperatures,  $\text{NH}_3$  is desorbed from the zeolite. A similar process is observed with the silazane/HY system by inspecting the IR spectra. The  $\text{NH}_4^-$  bending mode is diminished if the temperature is increased from 403 to 473 K. This shows how the byproduct of the anchoring reaction is removed from the zeolite.

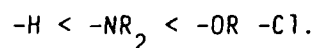
## CONCLUSION

The reactivity of functionalized silanes with the bridged hydroxyls within zeolitic pore systems has been investigated employing a combination of  $^{29}\text{Si}$  solid-state NMR and in situ IR techniques.

Due to their extreme acidity, the bridged zeolitic hydroxyls react in a fashion strikingly different from the behavior of terminal hydroxyls found at the surface of amorphous oxides. At moderate temperature, functional groups at the silane like  $-\text{OR}$ ,  $-\text{Cl}$ ,  $-\text{NR}_2$  or  $\text{H}$  are lost to form bridges to the zeolite framework. The reaction does not stop at this point, however.  $\text{Si}-\text{C}$  bonds are broken at elevated temperature, splitting off alkyl groups, and more highly substituted siloxane species are anchored to the framework.

The incorporation of silyl groups into the zeolite lattice could be considered as a model for early steps during the more severe lattice rearrangements observed upon reacting  $\text{SiCl}_4$  with an acid zeolite. In the latter case, framework aluminum atoms are substituted by silicon.

Based on the number of products and the reversibility of silane chemisorption, the reactivity of functional groups at Si with bridged zeolitic hydroxyls increases in the sequence:



If  $\text{Me}_3\text{Si}-\text{H}$ ,  $-\text{NR}_2$  or  $-\text{Cl}$  is reacted with the acidic zeolite, a product with a very unusual  $^{29}\text{Si}$  chemical shift at about +40 ppm is observed. Although no definitive assignment for this species can be given at this time, it is clear that an electronegative sigma-bonding ligand must be present at

the Si. The observations indicate either a strongly hydrogen-bonded silane with partial positive charge on the Si, or a silane-Lewis acid adduct, incorporated into the framework with a direct Si-metal bond.

Despite the complexity of the reactions considered, it is clear that bridged hydroxyls on solid surfaces are far more reactive than terminal hydroxyls.

The results of this study provide the basis for a systematic approach to modify and "functionalize" the internal surface of zeolitic cage systems. The work is being extended to reactive phosphorus compounds and results will be reported elsewhere.

#### ACKNOWLEDGEMENTS

The technical assistance of M.P. Stepro and D.E. Rothfuss is appreciated. The authors gratefully acknowledge discussions with Dr. D.B. Chase (DuPont), C.A. Fyfe (Guelph), and L. Baltusis (Varian).

## REFERENCES

- (1) Geismar, G.; Westphal, U. Z. anorg. allg. Chem., 1982, 484, 131.
- (2) McAteer, J.C.; Rooney, J.J. in "Molecular Sieves," Adv. Chem. Ser., 1973, 121, 258.
- (3) Barrer, R.M.; Trombe, J.C. JCS Faraday 1, 1978, 74, 2786.
- (4) Barrer, R.M.; Trombe, J.C. JCS Faraday 1, 1978, 74, 2798.
- (5) Barrer, R.M.; Vansant, E.F.; Peeters, G. JCS Faraday 1, 1978, 74, 1871.
- (6) Thijs, A.; Peeters, G.; Vansant, E.F.; Verhaert, I. JCS Faraday 1, 1983, 79, 2835.
- (7) Thijs, A.; Peeters, G.; Vansant, E.F.; Verhaert, I. JCS Faraday 1, 1983, 79, 2821.
- (8) Niwa, M.; Murakami, Y. Hyomen, 1984, 22, 319.
- (9) Rodewald, P.G. U.S. Pat. 4,402, 867, 1983.
- (10) Kerr, G.T. U.S. Pat. 3,682,996, 1972.
- (11) Gortsema, F.P.; Lok, B.M. Eur. Pat. appl. 0 100 544, 1983.
- (12) Kittelmann, U.; Diehl, M.; Bergmann, R.; Stadtmuller, G. U.S. Pat. 4,454,056, 1984.
- (13) Campbell, T.C. et al., U.S. Pat. 4,216,125, 1980.
- (14) Hertenzenberg, E.P. et al., U.S. Pat. 4,138,363, 1979.
- (15) Sindorf, D.W.; Maciel, G.E. J. Phys. Chem., 1983, 87, 5516.
- (16) Sindorf, D.W.; Maciel, G.E. J. Am. Chem. Soc., 1983, 105, 1487.
- (17) Sindorf, D.W.; Maciel, G.E. J. Phys. Chem. 1982, 86, 5208.
- (18) Maciel, G.E.; Sindorf, D.W.; Bartuska, V.J. J. Chromatogr., 1981, 205, 438.
- (19) Sindorf, D.W.; Maciel, G.E. J. Am. Chem. Soc., 1981, 103, 4263.
- (20) Maciel, G.E.; Sindorf, D.W. J. Am. Chem. Soc., 1980, 102, 7606.
- (21) Kohler, J.; Chase, D.B.; Farlee, R.D.; Vega, A.J.; Kirkland, J.J. J. Chromatogr., 1986, 352, 275.
- (22) Miller, M.L.; Linton, R.W.; Maciel, G.E.; Hawkins, B.L. J. Chromatogr. 1985, 319, 9.



- (23) Bayer, E.; Albert, K.; Reiners, J.; Nieder, M.; J. Chromatogr., 1983, 264, 197.
- (24) Hertl, W.; Hair, M.L. J. Phys. Chem., 1971, 76, 2181.
- (25) Hertl, W. J. Phys. Chem., 1968, 72, 1248.
- (26) Ernst, C.R.; Spailter, L.; Buell, G.R.; Wilhite, D.L. J. Am. Chem. Soc., 1974, 96, 5375.
- (27) Sindorf, D.W.; Maciel, G.E. J. Am. Chem. Soc., 1983, 105, 3767.
- (28) Janes, N.; Oldfield, E. J. Am. Chem. Soc., 1985, 107, 6769.
- (29) Harris, R.K.; Kennedy, J.D.; McFarlane, W. Chapt. 10 in "NMR and the Periodic Table," ed. R.K. Harris, B.E. Mann, Academic Press, 1978.
- (30) Harris, R.K.; Knight, C.T.G.; Hull, W.E. J. Am. Chem. Soc., 1981, 103, 1577.
- (31) Marsmann, H.C.; Meyer, E.; Vongehr, M.; Weber, E.F. Makromol. Chem., 1983, 184, 1817.
- (32) Magi, M.; Lippmaa, E.; Samosan, A.; Englehardt, G.; Grimmer, A.-R. J. Phys. Chem., 1984, 88, 1518.
- (33) Ramdas, S.; Klinowski, J. Nature, 1984, 308, 521.
- (34) Williams, E.A. Annu. Rep. NMR Spectros., 1983, 15, 235.
- (35) Bein, T.; Chase, D.B.; Farlee, R.D.; Stucky, G.D. Proc. 7th Internat. Zeolite Conf., Tokyo, 1986, ed. Y. Murakami, A. Iijima, J.W. Ward, Kodansha: Tokyo, 1986, p. 311.
- (36) Sefcik, M.D.; Henis, J.M.S.; Gaspar, P.P. J. Chem. Phys., 1974, 4329.
- (37) Schleyer, P.R.; Apeloig, Y.; Arad, D.; Luke, B.T.; Pople, J.A. Chem. Phys. Lett., 1983, 95, 477.

### Figure Captions.

Figure 1-4.  $^{29}\text{Si}$  CP-MAS NMR spectra of trimethylmethoxysilane chemisorbed on dehydrated HY zeolite. X denotes spinning sidebands of the zeolite framework resonances.

Figure 1, equilibrated for 120 min at 295 K, degassed for 30 min. (2.4 equivalents per supercage, 2.4/SC).

Figure 2, degassed at 403 K for 180 min.

Figure 3, degassed at 523 K for 12 hrs.

Figure 4, equilibrated at 473 K for 120 min, degassed for 30 min. (2.4/SC).

Figure 5. IR spectra of a wafer of HY zeolite, degassed at 670 K, loaded with  $\text{Me}_3\text{SiOMe}$ .

A, the degassed zeolite.

B, equilibrated for 10 min at 295 K, degassed for 30 min.

C, equilibrated for 60 min at 403 K, degassed for 10 min.

D, equilibrated for 120 min at 473 K, degassed for 10 min.

Figure 6-7.  $^{29}\text{Si}$  CP-MAS NMR spectra of methyltrimethoxysilane chemisorbed on dehydrated HY zeolite.

Figure 6, equilibrated for 120 min at 295 K, degassed for 30 min. (0.3/SC).

Figure 7, degassed at 403 K for 180 min. (<0.1/SC).

Figure 8. IR spectra of a wafer of HY zeolite, degassed at 670 K, loaded with  $\text{MeSi(OMe)}_3$ .

A, the degassed zeolite.

B, equilibrated for 10 min at 295 K, degassed for 30 min.

C, equilibrated for 60 min at 403 K, degassed for 10 min.

D, equilibrated for 120 min at 473 K, degassed for 10 min.

Figure 9-12.  $^{29}\text{Si}$  CP-MAS NMR spectra of trimethylchlorosilane chemisorbed on dehydrated HY zeolite. X denotes spinning sidebands from the zeolite framework resonances.

Figure 9, equilibrated for 120 min at 295 K, degassed for 30 min. (1.2/SC).

Figure 10, degassed for 180 min at 403 K. (<0.2/SC).

Figure 11, equilibrated for 120 min at 473 K, degassed for 30 min. (2.1/SC).

Figure 12, dehydrated NaY zeolite, equilibrated with the silane at 295 K for 120 min, degassed for 30 min. (2.8/SC).

Figure 13. IR spectra of a wafer of HY zeolite, degassed at 670 K, loaded with  $\text{Me}_3\text{SiCl}$ .

A, the degassed zeolite.

B, equilibrated for 10 min at 295 K, degassed for 30 min.

C, equilibrated for 60 min at 403 K, degassed for 10 min.

D, equilibrated for 120 min at 473 K, degassed for 10 min.

Figure 14 and 16.

$^{29}\text{Si}$  CP-MAS NMR spectra of silanes chemisorbed on dehydrated HY zeolite.

Figure 14, hexamethyldisilazane equilibrated for 120 min at 473 K, degassed for 30 min. (0.4/SC).

Figure 16, trimethylsilane equilibrated for 120 min at 473 K, degassed for 30 min. (1.8/SC).

Figure 15. IR spectra of a wafer of HY zeolite, degassed at 670 K, loaded with  $(\text{Me}_3\text{Si})_2\text{NH}$ .

A, the degassed zeolite.

B, equilibrated for 10 min at 295 K, degassed for 30 min.

C, equilibrated for 60 min at 403 K, degassed for 10 min.

D, equilibrated for 120 min at 473 K, degassed for 10 min.

Figure 17. IR spectra of a wafer of HY zeolite, degassed at 670 K, loaded with  $\text{Me}_3\text{SiH}$ .

A, the degassed zeolite.

B, equilibrated for 10 min at 295 K, with gas phase silane.

C, sample B, degassed for 30 min at 295 K.

D, equilibrated for 60 min at 403 K, with gas phase silane.

E, sample D, degassed for 30 min at 403 K.

Table I.  $^{29}\text{Si}$  Chemical Shifts of Substituted Methylsilanes

<u>Molecule or Site</u>	<u>Shift<sup>a</sup></u>
Monosubstituted	
$\text{Me}_3\text{SiCl}$	+30 <sup>b</sup>
$\text{Me}_3\text{SiOMe}$	+18 <sup>b</sup>
$\text{Me}_3\text{SiOH}$	+17 <sup>c</sup>
$\text{Me}_3\text{SiOSi}$	+8 <sup>d</sup>
$\text{Me}_3\text{SiH}$	-16 <sup>b</sup>
Disubstituted	
$\text{Me}_2\text{SiCl}_2$	+32 <sup>b</sup>
$\text{Me}_2\text{Si}(\text{Cl})\text{OSi}$	+2 <sup>d</sup>
$\text{Me}_2\text{Si}(\text{OMe})_2$	-2 <sup>b</sup>
$\text{Me}_2\text{Si}(\text{OH})\text{OSi}$	-12 <sup>d</sup>
$\text{Me}_2\text{Si}(-\text{OSi})_2$	-14 <sup>d</sup>
Trisubstituted	
$\text{MeSiCl}_3$	+12 <sup>b</sup>
$\text{MeSi}(\text{Cl})_2\text{OSi}$	-14 <sup>d</sup>
$\text{MeSi}(\text{Cl})(\text{OSi})_2$	-38 <sup>d</sup>
$\text{MeSi}(\text{Cl})(\text{OH})(\text{OSi})$	-29 <sup>d</sup>
$\text{MeSi}(\text{OMe})_3$	-41 <sup>b</sup>
$\text{MeSi}(\text{OH})_2(\text{OSi})$	-42 <sup>d</sup>
$\text{MeSi}(\text{OH})(\text{OSi})_2$	-52 <sup>d</sup>
$\text{MeSi}(\text{OMe})(\text{OSi})_2$	-58 <sup>c</sup>
$\text{MeSi}(\text{OSi})_3$	-62 <sup>d</sup>
Quaternary	
$\text{Si}(\text{OMe})_4$	-79 <sup>b,e</sup>
$\text{Si}(\text{OMe})_3(\text{OSi})$	-86 <sup>e</sup>
$\text{Si}(\text{OMe})_2(\text{OSi})_2$	-94 <sup>e</sup>
$\text{Si}(\text{OMe})(\text{OSi})_3$	-104 <sup>e</sup>
$\text{Si}(\text{OH})_4$	-74 <sup>f</sup>
$\text{Si}(\text{OH})_3(\text{OSi})$	-83 <sup>g,h</sup>
$\text{Si}(\text{OH})_2(\text{OSi})_2$	-92 <sup>h,i</sup>
$\text{Si}(\text{OH})(\text{OSi})_3$	-104 <sup>h,i</sup>
$\text{Si}(\text{OSi})_4$	-112 <sup>h,i,j</sup>

Table I, continued.

- a in ppm relative to  $\text{Me}_4\text{Si}$ .
- b Table 10.1, p. 313, in ref. 29.
- c predicted using additive substituent effects from data in ref. 29, following the method outlined in ref. 27 as further discussed in the text.
- d ref. 27.
- e ref. 31
- f R.D. Farlee, T.P. Concannon, unpublished work; similar values have been reported elsewhere (refs. 28,30).
- g Average value for disilicates.
- h Analogous sites in silicates exhibit chemical shifts covering a substantial range (ref. 32) depending on the average substituent electronegativity and Si-O-Si angle (ref. 28).
- i These are typical values for silica (refs. 21,27).
- j Q4 sites in zeolites and tectosilicates span a considerable range and can be predicted from the number of Al neighbors and average Si-O-T (T = Si,Al) angle (ref. 33).

TABLE II.

<sup>29</sup>Si CP-MAS Resonances Observed after Adsorption of  
Trimethylmethoxysilane, Me<sub>3</sub>SiOMe, on H-Y Zeolite.

<u>Conditions</u>	<u>Assignment</u>	<u>Shift</u>	<u>Mole %</u>
vapor 295 K, 120 min., degassed 30 min.	Lewis-adduct	31 ppm	17
	Me <sub>3</sub> SiOMe	20	45
	Me <sub>3</sub> SiOSi	10	38
degassed 403 K, 180 min.	Me <sub>2</sub> Si(OMe) <sub>2</sub>	0	28
	Me <sub>2</sub> Si(OMe)OSi	-11	54
	Me <sub>2</sub> Si(OSi) <sub>2</sub>	-20	18
degassed 523 K, 12 hrs.	Me <sub>2</sub> Si(OMe) <sub>2</sub>	0	23
	Me <sub>2</sub> Si(OMe)OSi	-11	29
	Me <sub>2</sub> Si(OSi) <sub>2</sub>	-19	48
	MeSi(OMe)(OSi) <sub>2</sub>	-56	
vapor 473 K, 120 min., degassed 10 min.	Me <sub>2</sub> Si(OMe) <sub>2</sub>	1	18
	Me <sub>2</sub> Si(OSi) <sub>2</sub>	-18	32
	MeSi(OMe) <sub>2</sub> OSi	-39	9
	MeSi(OMe)(OSi) <sub>2</sub>	-57	41

TABLE III.

$^{29}\text{Si}$  CP-MAS Resonances Observed after Adsorption of Methyltrimethoxysilane,  $\text{MeSi}(\text{OMe})_3$ , on H-Y Zeolite.

<u>Conditions</u>	<u>Assignment</u>	<u>Shift</u>	<u>Mole %</u>
vapor 295 K, 10 min., degassed 30 min.	$\text{Me}_3\text{SiOMe}$	18	7
	$\text{Me}_3\text{SiOSi}$	8	7
	$\text{MeSi}(\text{OMe})_3$	-38	14
	$\text{MeSi}(\text{OMe})_2\text{OSi}$	-46	53
	$\text{MeSi}(\text{OMe})(\text{OSi})_2$	-57	19
degassed 403 K, 180 min.	$\text{Me}_3\text{SiOSi}$	12	21
	$\text{MeSi}(\text{OMe})_2\text{OSi}$	-45	25
	$\text{MeSi}(\text{OMe})(\text{OSi})_2$	-56	53

TABLE IV.

<sup>29</sup>Si CP-MAS Resonances Observed after Adsorption of  
Trimethylchlorosilane, Me<sub>3</sub>SiCl, on H-Y and Na-Y Zeolites.

<u>Conditions</u>	<u>Assignment</u>	<u>Shift</u>	<u>Mole %</u>
H-Y			
vapor 295 K, 120 min., degassed 30 min.	Lewis-adduct	40	17
	Me <sub>3</sub> SiOH	21	42
	Me <sub>3</sub> SiOSi	12	24
	Me <sub>2</sub> Si(OSi) <sub>2</sub>	-5,-10	17
degassed 403 K, 180 min.	Lewis-adduct	41	12
	Me <sub>3</sub> SiCl	27	17
	Me <sub>3</sub> SiOH	21	9
	Me <sub>3</sub> SiOSi	13	28
	Me <sub>2</sub> Si(OH)OSi	-9	34
vapor 473 K, 120 min., degassed 30 min.	Me <sub>3</sub> SiOSi	7	37
	Me <sub>2</sub> Si(OH)(OSi)	-11,-14	33
	MeSi(OH)(OSi) <sub>2</sub>	-53	15
	MeSi(OSi) <sub>3</sub>	-59	15
Na-Y			
vapor 295 K, 120 min., degassed 30 min.	Lewis-adduct	38	71
	Me <sub>3</sub> SiOMe	18	14
	Me <sub>3</sub> SiOSi	6	9



TABLE V.

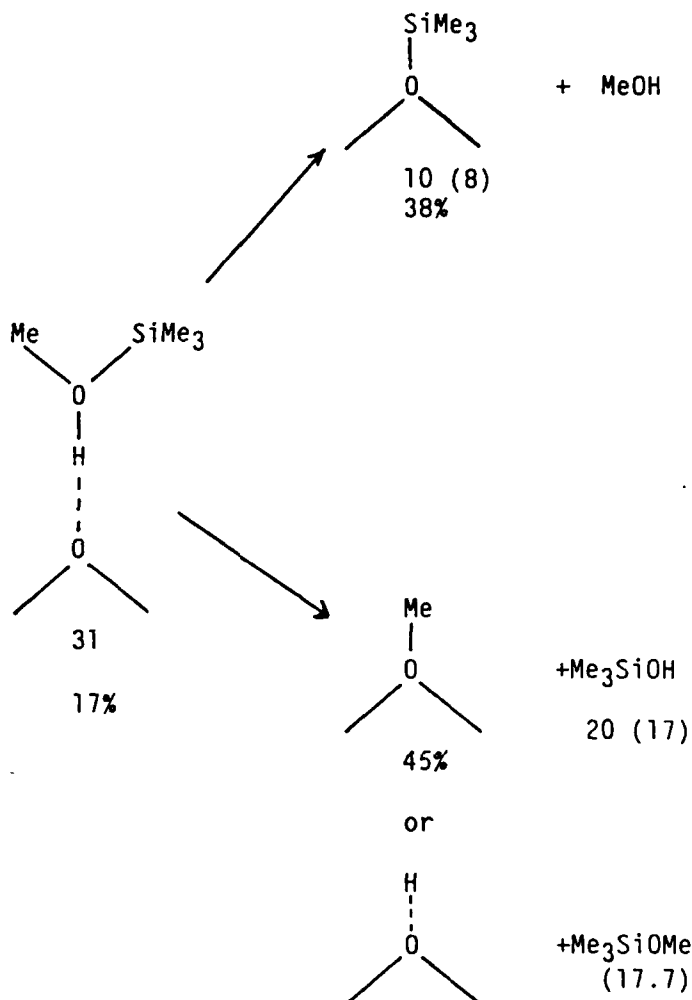
$^{29}\text{Si}$  CP-MAS Resonances Observed after Adsorption of  
Trimethylsilane,  $\text{Me}_3\text{SiH}$ , or Hexamethyldisilazane,  $(\text{Me}_3\text{Si})_2\text{NH}$ ,  
on H-Y Zeolite.

<u>Silane, conditions</u>	<u>Assignment</u>	<u>Shift</u>	<u>Mole %</u>
$\text{Me}_3\text{SiH}$			
vapor 473 K, 120 min., degassed 30 min.	Lewis-adduct	41	60
	$\text{Me}_2\text{Si}(\text{OMe})_2$	-2	40
$(\text{Me}_3\text{Si})_2\text{NH}$			
vapor 473 K, 120 min., degassed 30 min.	Lewis-adduct	41	38
	$\text{Me}_3\text{SiOSi}$	10	33
	$\text{Me}_2\text{Si}(\text{OSi})_2$	-14	27

Me<sub>3</sub>SiOMe    295 K

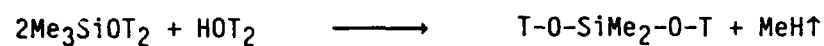
Me<sub>3</sub>SiOMe

17.7



Scheme 1. Proposed Reaction Pathways for Me<sub>3</sub>SiOMe in HY Zeolite at 295 K. Indicated values are the <sup>29</sup>Si chemical shift data, compared to expected values (Table 1) in parentheses. Per cent values refer to the relative amounts of silane species as detected by <sup>29</sup>Si MAS-NMR.

Me<sub>3</sub>SiOMe    403K

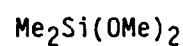


-20 (-14)

18%



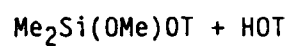
MeOH



0 (-2)

28%

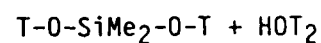
MeOH



-11 (-12)

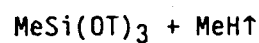
54%

473K



-18 (-14)

32%



-57 (-62)

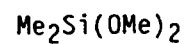
or



(-58)

41%

and



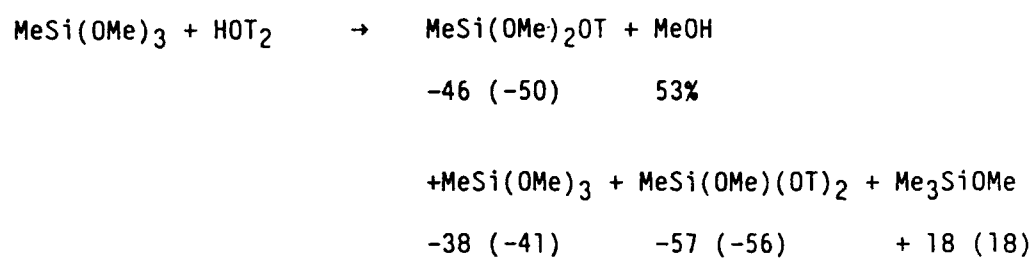
1 (-2)

18%

Scheme 2. Proposed Reaction Pathways for Me<sub>3</sub>SiOMe in HY Zeolite at Elevated Temperatures

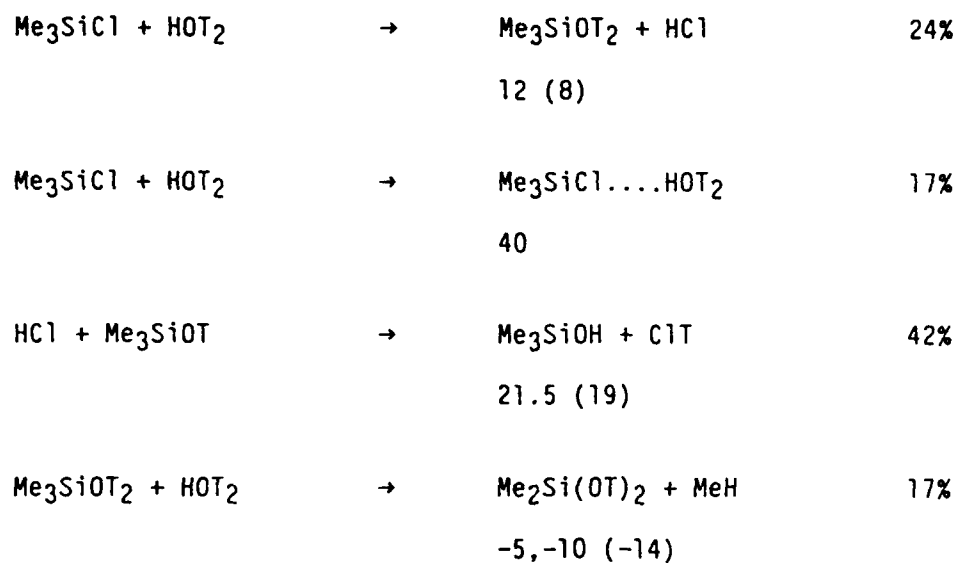
MeSi(OMe)<sub>3</sub> 295K

---



Scheme 3. Proposed Reaction Pathways for MeSi(OMe)<sub>3</sub> in HY Zeolite at 295 K

Me<sub>3</sub>SiCl 295 K

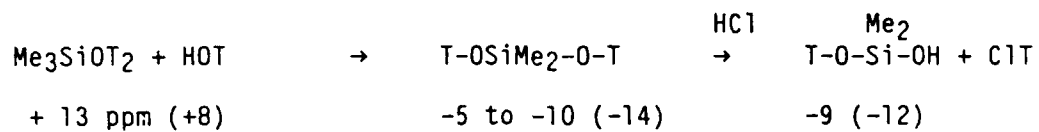


Scheme 4. Proposed Reaction Pathways for Me<sub>3</sub>SiCl in HY Zeolite at

A) 295 K

B) elevated temperatures

Me<sub>3</sub>SiCl 403 K

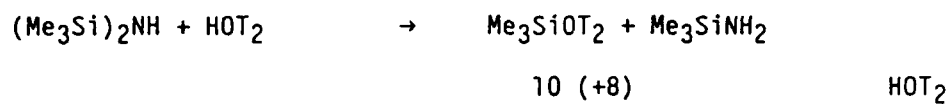


473K

7 ppm	-11 ppm	-53 to -59 ppm
37%	33%	30%
Mono-	Di-	Tri-substituted

Scheme 4 B.

(Me<sub>3</sub>Si)<sub>2</sub>NH 473



T-O-SiMe<sub>2</sub>OT

-14 (-14)

Me<sub>3</sub>SiN<sup>+</sup>H<sub>3</sub>OT<sub>2</sub>

41

38%

Scheme 5. Proposed Reaction Pathways for (Me<sub>3</sub>Si)<sub>2</sub> NH in HY Zeolite at 473 K

Me<sub>3</sub>SiOMe on HY Zeolite

<sup>29</sup>Si CP-MAS NMR

Fig. 4A: adsorbed at 473 K

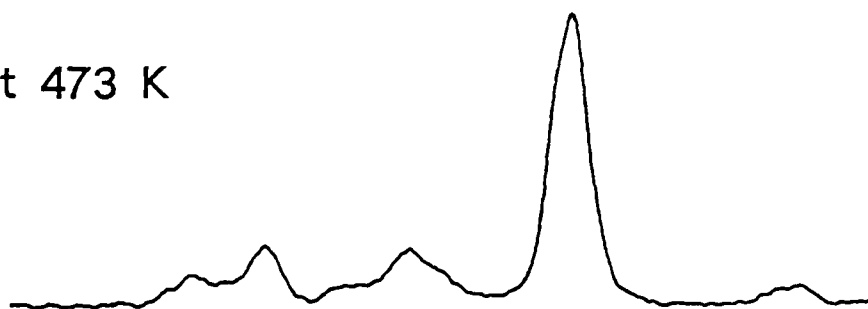


Fig. 3A: degassed at 523 K



Fig. 2A: degassed at 403 K



Fig. 1A: adsorbed at 295 K



0.0

-100.0

PPM



Me<sub>3</sub>SiOMe on HY Zeolite

<sup>29</sup>Si CP-MAS NMR

Fig. 4B: adsorbed at 473 K

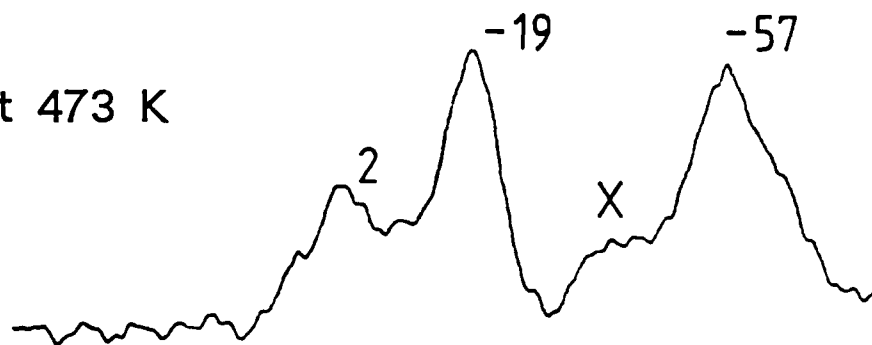


Fig. 3B: degassed at 523 K

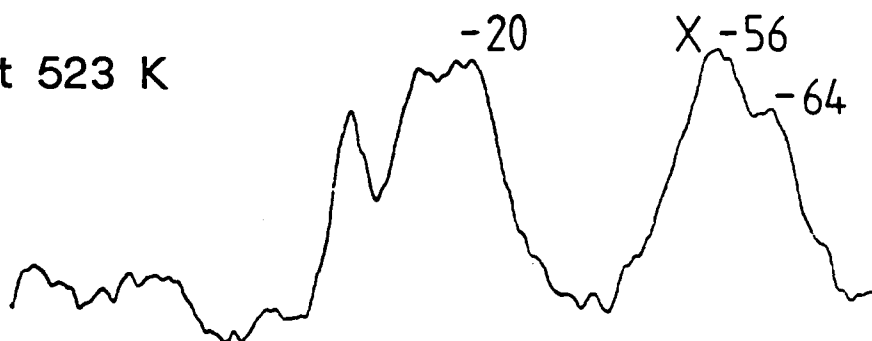


Fig. 2B: degassed at 403 K

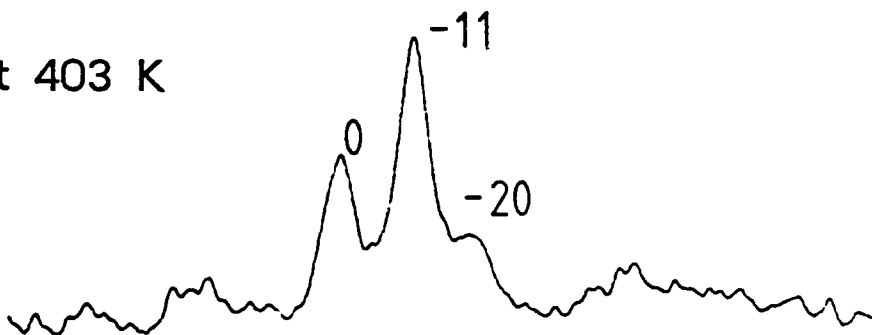


Fig. 1B: adsorbed at 295 K

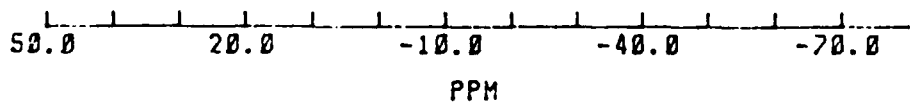
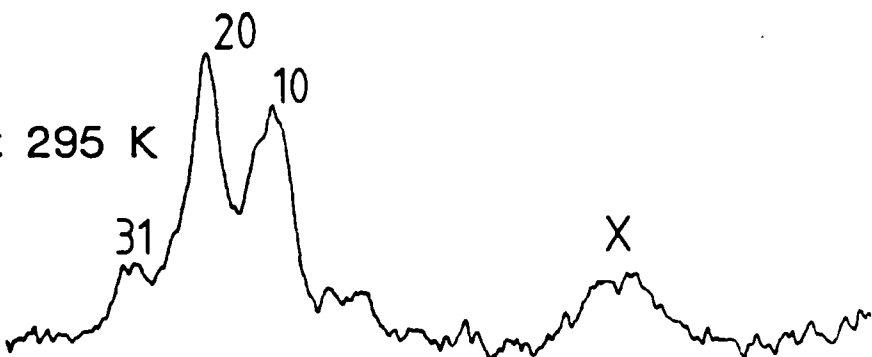
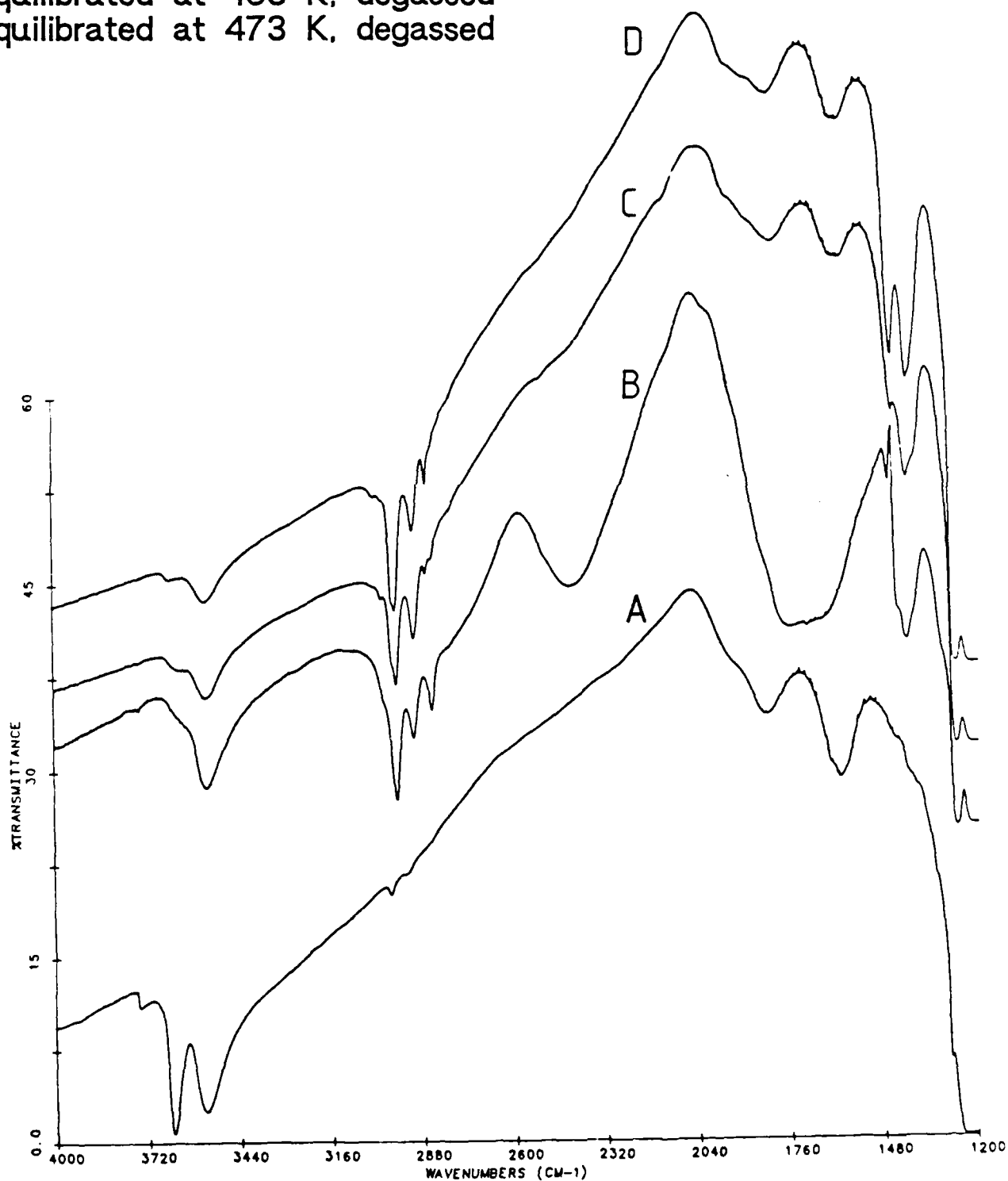


Fig. 5: In Situ IR Spectra

$\text{Me}_3\text{SiOMe}$  on HY Zeolite

- A, degassed zeolite
- B, equilibrated at 295 K, degassed
- C, equilibrated at 403 K, degassed
- D, equilibrated at 473 K, degassed



MeSi(OMe)<sub>3</sub> on HY Zeolite

<sup>29</sup>Si CP-MAS NMR

Fig. 7A: degassed at 403 K

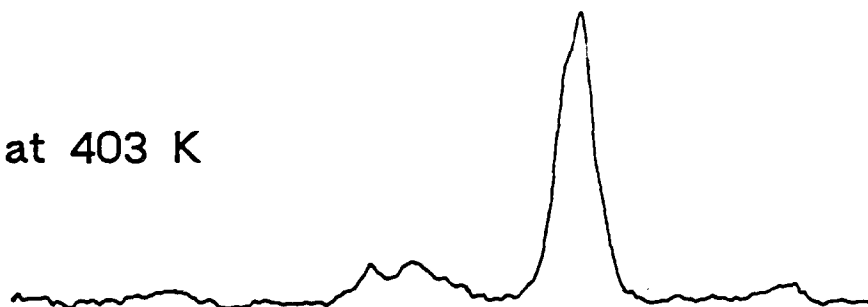
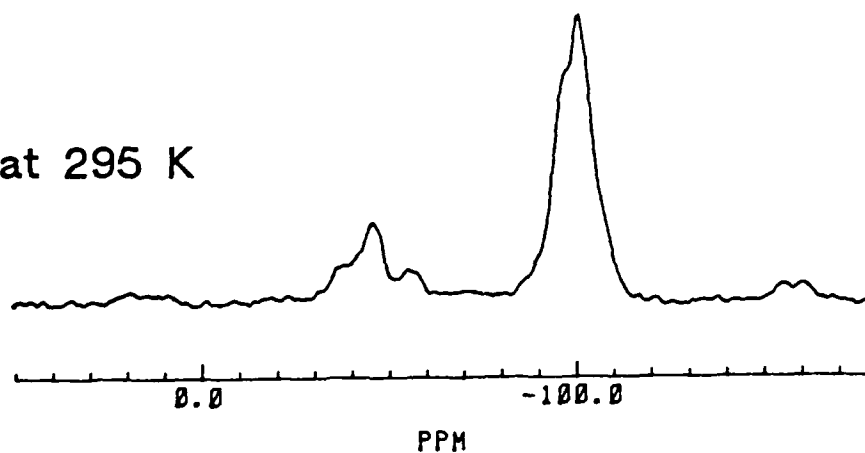


Fig. 6A: adsorbed at 295 K



MeSi(OMe)<sub>3</sub> on HY Zeolite

<sup>29</sup>Si CP-MAS NMR

Fig. 7B: degassed at 403 K

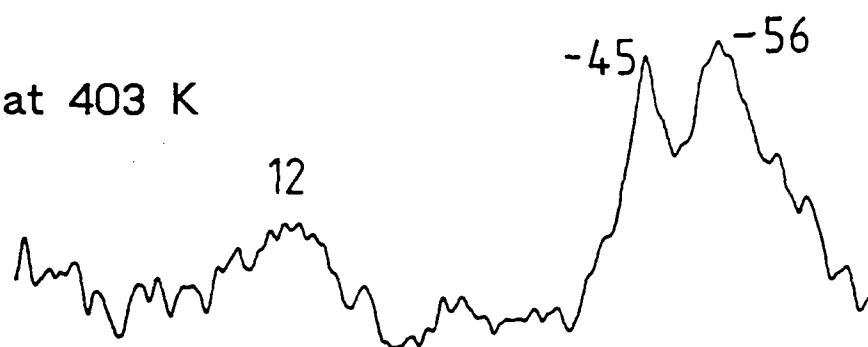


Fig. 6B: adsorbed at 295 K

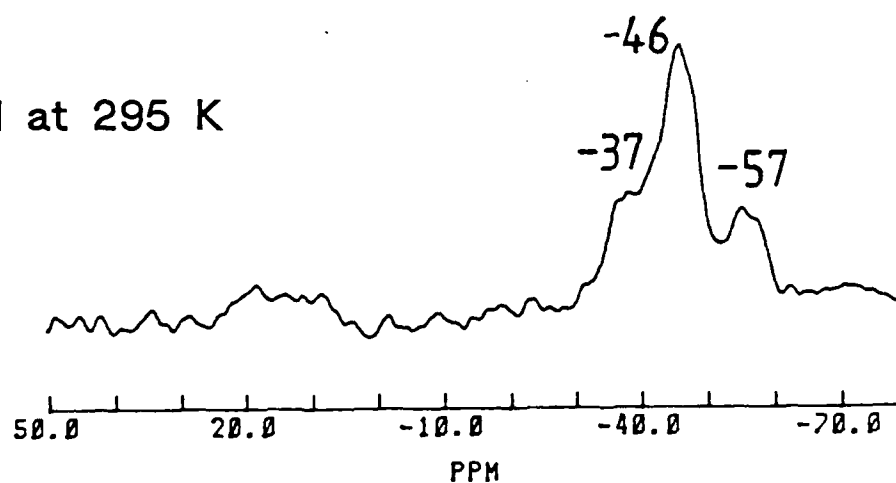


Fig. 8: In Situ IR Spectra

$\text{MeSi(OMe)}_3$  on HY Zeolite

A, degassed zeolite

B, equilibrated at 295 K, degassed

C, equilibrated at 403 K, degassed

D, equilibrated at 473 K, degassed

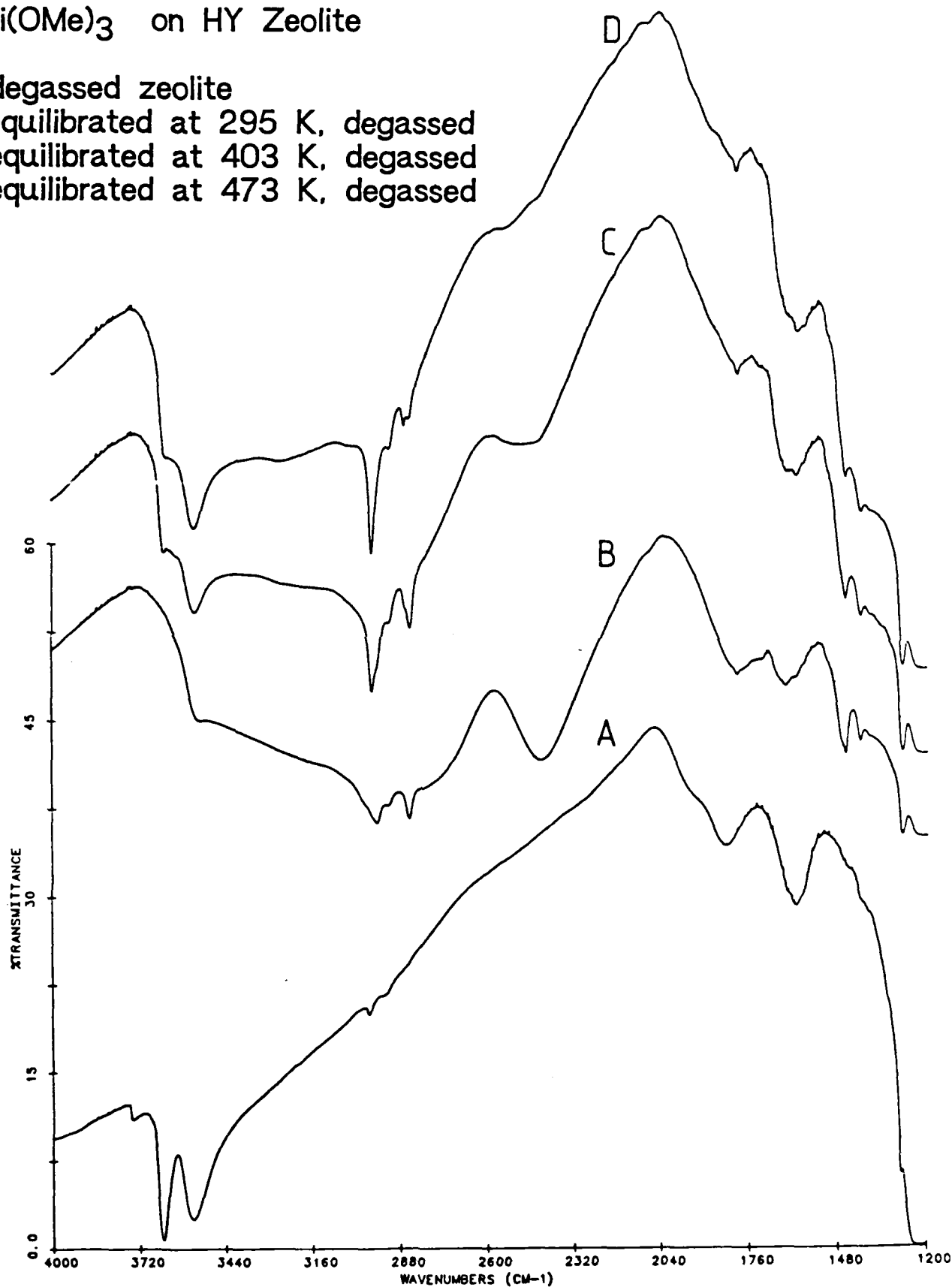


Fig. 12A: on NaY, adsorbed at 295 K

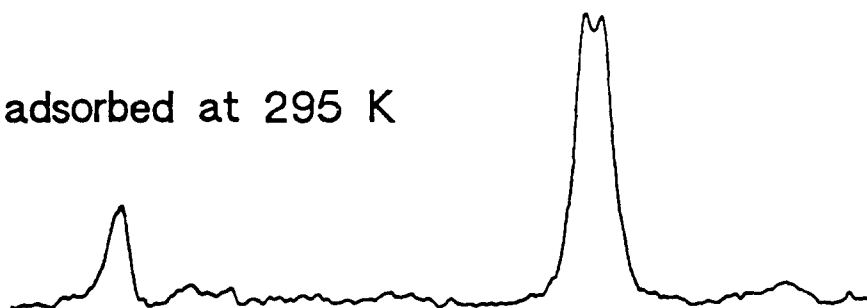


Fig. 11A: on HY, adsorbed at 473 K

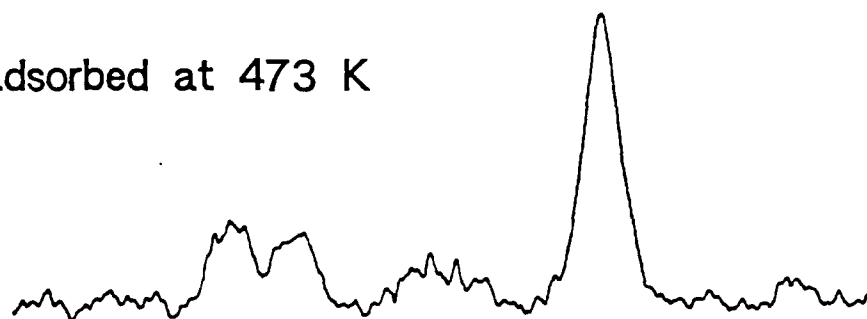


Fig. 10A: on HY, degassed at 403 K

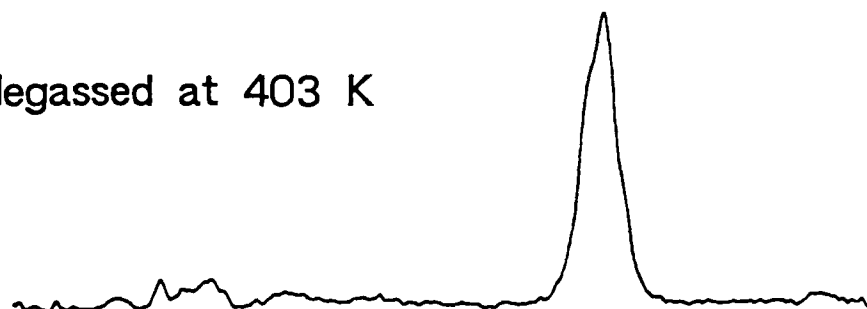


Fig. 9A: on HY, adsorbed at 295 K

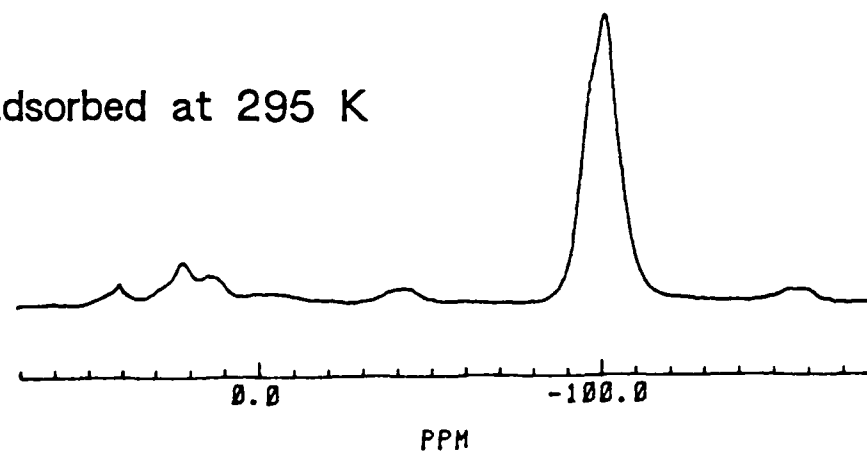


Fig. 12B: on NaY,  
adsorbed at 295 K

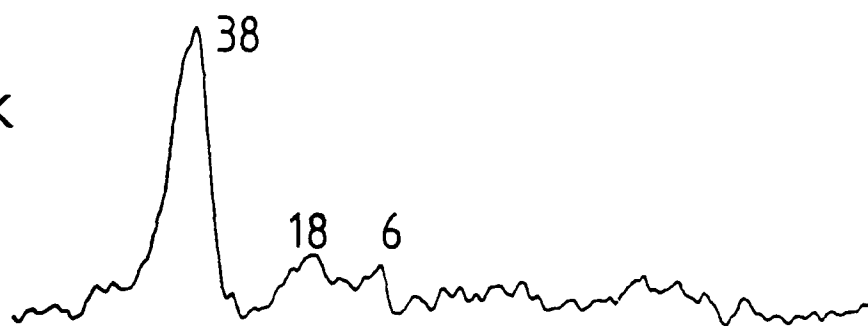


Fig. 11B: on HY,  
adsorbed at 473 K

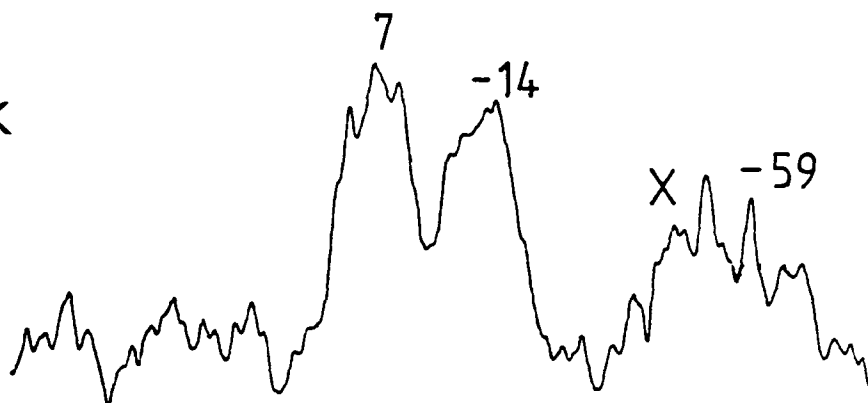


Fig. 10B: on HY,  
degassed at 403 K

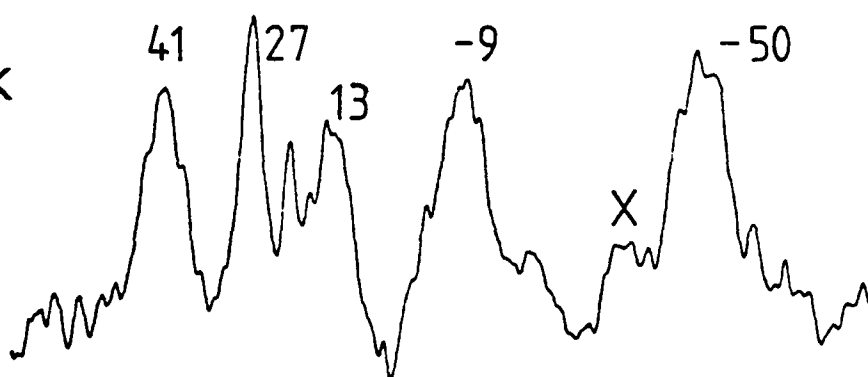


Fig. 9B: on HY,  
adsorbed at 295 K

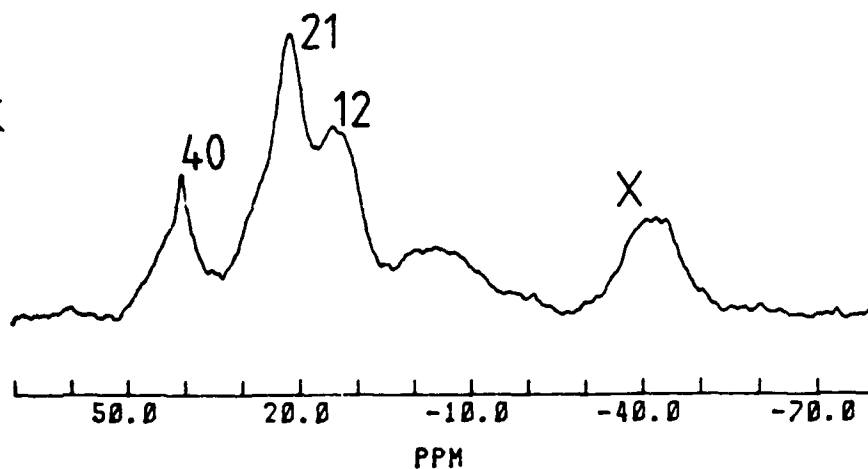


Fig. 13: In Situ IR Spectra

$\text{Me}_3\text{SiCl}$  on HY Zeolite

- A, degassed zeolite
- B, equilibrated at 295 K, degassed
- C, equilibrated at 403 K, degassed
- D, equilibrated at 473 K, degassed

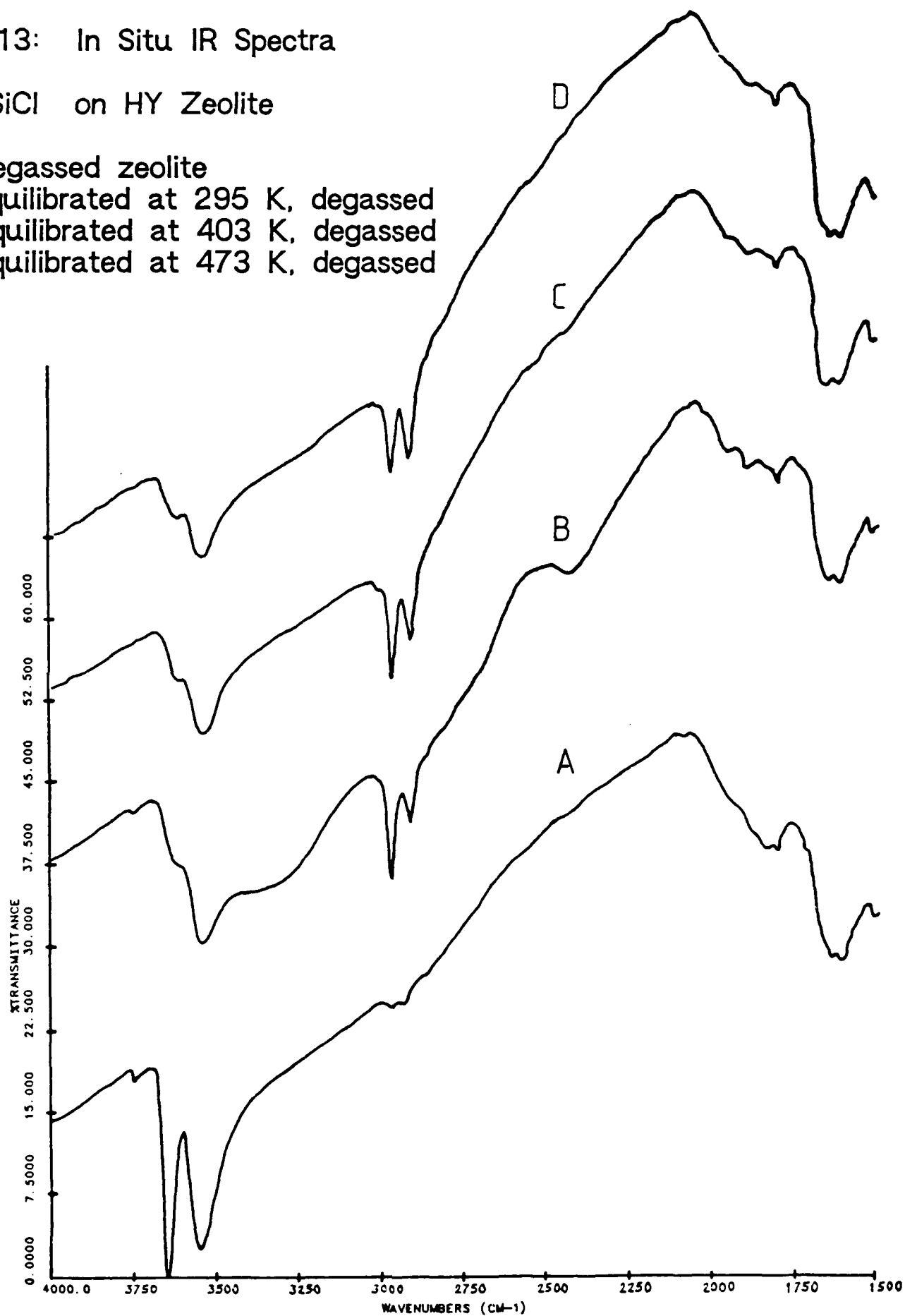




Fig. 16A:  $\text{Me}_3\text{SiH}$   
adsorbed at 473 K

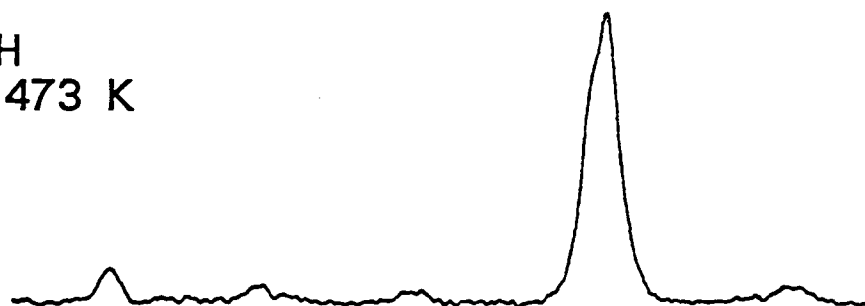


Fig. 14A:  $(\text{Me}_3\text{Si})_2\text{NH}$   
adsorbed at 473 K

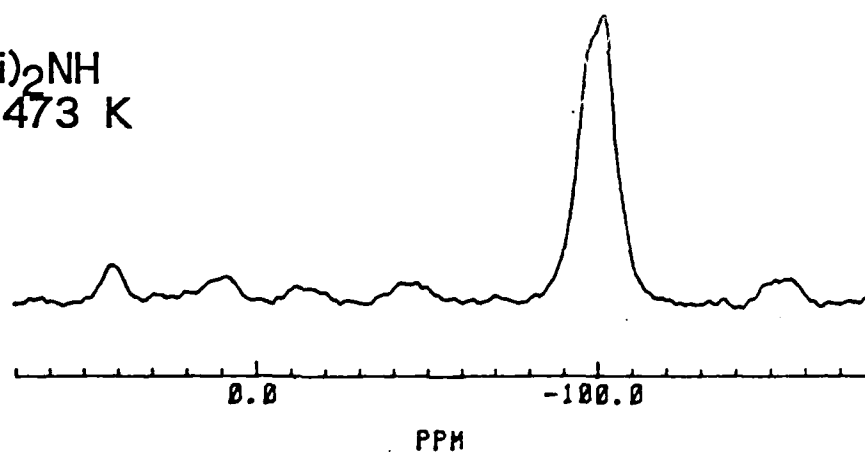


Fig. 16B:  $\text{Me}_3\text{SiH}$   
adsorbed at 473 K

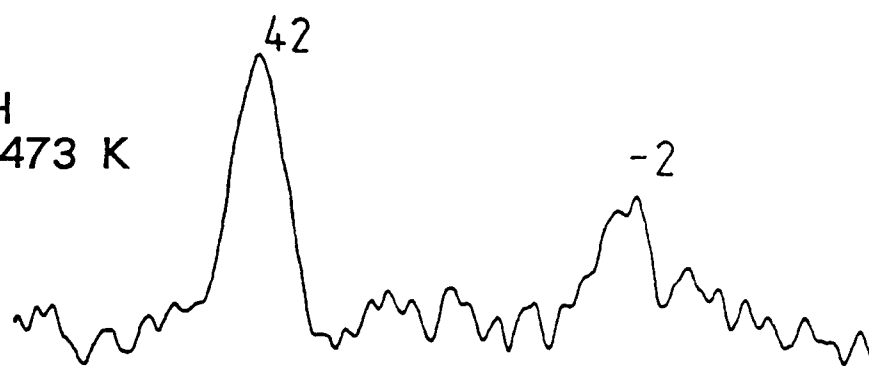


Fig. 14B:  $(\text{Me}_3\text{Si})_2\text{NH}$   
adsorbed at 473 K

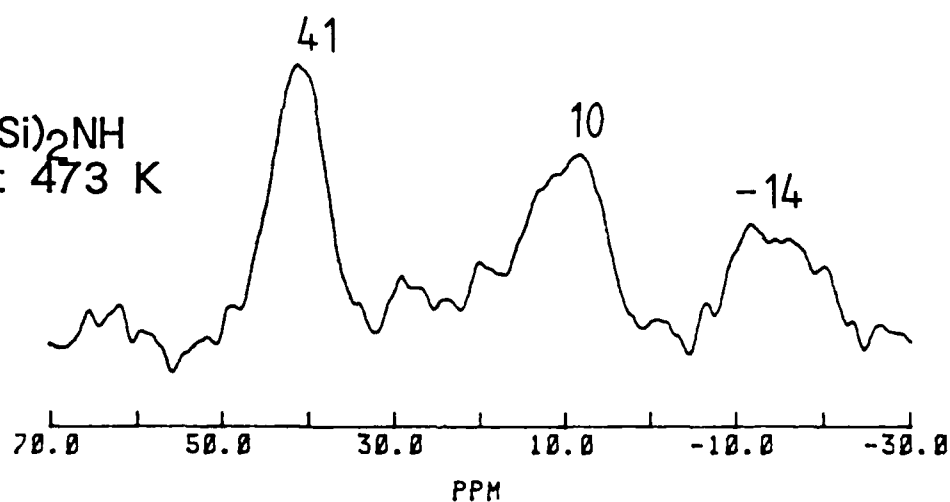


Fig. 15: In Situ IR Spectra

$(\text{Me}_3\text{Si})_2\text{NH}$  on HY Zeolite

A, degassed zeolite

B, equilibrated at 295 K, degassed

C, equilibrated at 403 K, degassed

D, equilibrated at 473 K, degassed

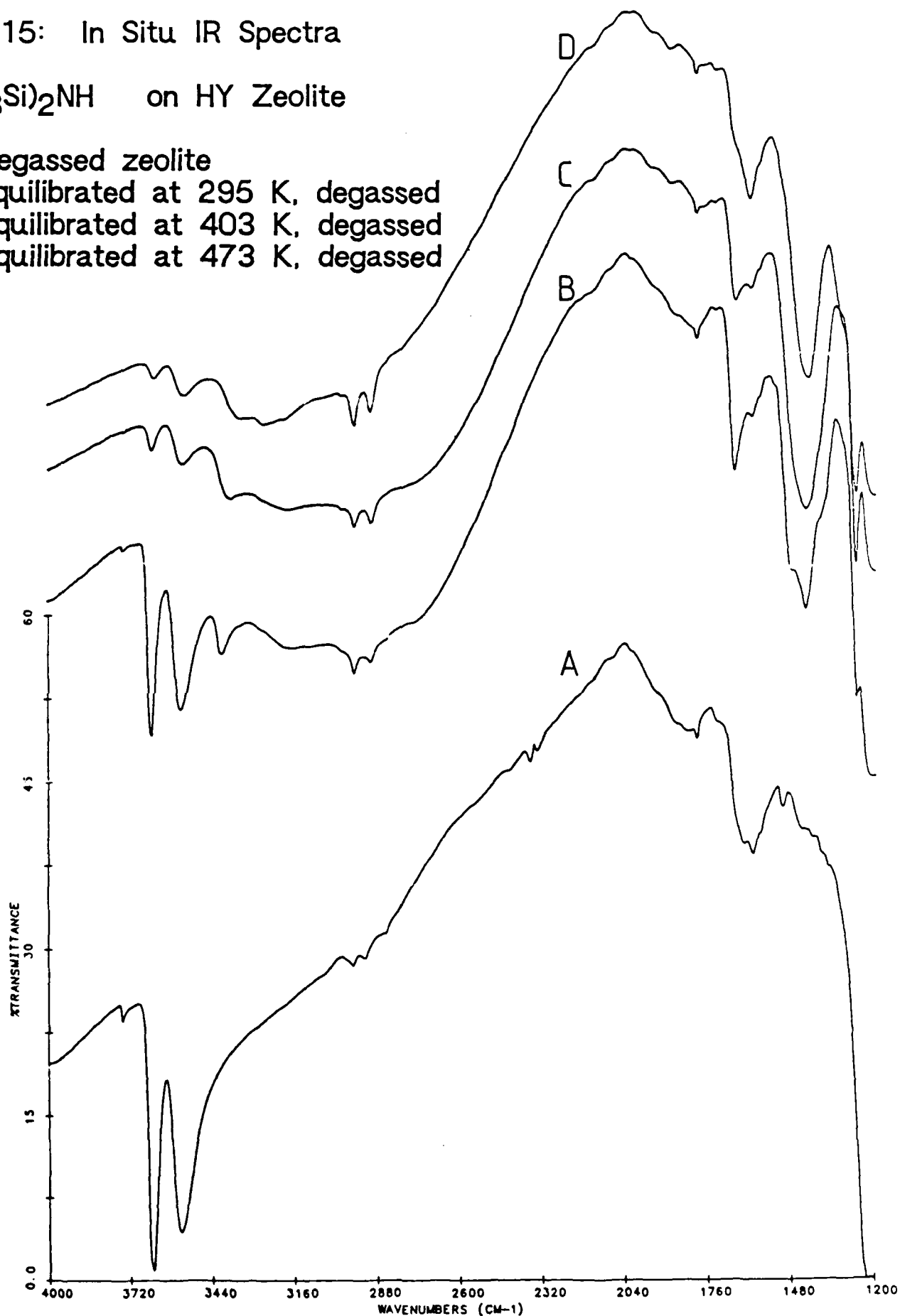


Fig. 17: In Situ IR Spectra

$\text{Me}_3\text{SiH}$  on HY Zeolite

- A, degassed zeolite
- B, equilibrated at 295 K, gas phase silane
- C, degassed at 295 K
- D, equilibrated at 403 K, gas phase silane
- E, degassed at 403 K

